

# Mitochondria transfer-based therapies reduce the morbidity and mortality of Leigh syndrome

Received: 21 August 2023

Accepted: 8 August 2024

Published online: 2 September 2024

 Check for updates

A list of authors and their affiliations appears at the end of the paper

Mitochondria transfer is a recently described phenomenon in which donor cells deliver mitochondria to acceptor cells<sup>1–3</sup>. One possible consequence of mitochondria transfer is energetic support of neighbouring cells; for example, exogenous healthy mitochondria can rescue cell-intrinsic defects in mitochondrial metabolism in cultured  $\rho^0$  cells or *Ndufs4*<sup>-/-</sup> peritoneal macrophages<sup>4–7</sup>. Exposing haematopoietic stem cells to purified mitochondria before autologous haematopoietic stem cell transplantation allowed for treatment of anaemia in patients with large-scale mitochondrial DNA mutations<sup>8,9</sup>, and mitochondria transplantation was shown to minimize ischaemic damage to the heart<sup>10–12</sup>, brain<sup>13–15</sup> and limbs<sup>16</sup>. However, the therapeutic potential of using mitochondria transfer-based therapies to treat inherited mitochondrial diseases is unclear. Here we demonstrate improved morbidity and mortality of the *Ndufs4*<sup>-/-</sup> mouse model of Leigh syndrome (LS) in multiple treatment paradigms associated with mitochondria transfer. Transplantation of bone marrow from wild-type mice, which is associated with release of haematopoietic cell-derived extracellular mitochondria into circulation and transfer of mitochondria to host cells in multiple organs, ameliorates LS in mice. Furthermore, administering isolated mitochondria from wild-type mice extends lifespan, improves neurological function and increases energy expenditure of *Ndufs4*<sup>-/-</sup> mice, whereas mitochondria from *Ndufs4*<sup>-/-</sup> mice did not improve neurological function. Finally, we demonstrate that cross-species administration of human mitochondria to *Ndufs4*<sup>-/-</sup> mice also improves LS. These data suggest that mitochondria transfer-related approaches can be harnessed to treat mitochondrial diseases, such as LS.

LS is a primary mitochondrial disease characterized by progressive neurological deficits, muscle weakness, ataxia and respiratory failure<sup>17</sup>. Unfortunately, there are no therapies for LS, and the majority of children affected by this disease die by the age of 3 years old<sup>18</sup>. This disease is characterized by mutations in 113 genes that affect electron transport chain function, with one commonly affected gene being *NDUFS4*, a nuclear (n)DNA-encoded enzyme that is required for complex I assembly and function<sup>19</sup>. Mice with a loss-of-function mutation

in *Ndufs4* exhibit many of the features of LS and die within the first 2 months of life<sup>20</sup>. We hypothesized that engraftment of a wild-type (WT) haematopoietic system in *Ndufs4*<sup>-/-</sup> mice would provide a systemically distributed, durable supply of healthy cells that could transfer their mitochondria to diseased cells to reduce the morbidity and mortality of LS.

To begin investigating this, we lethally irradiated 3–5-week-old *Ndufs4*<sup>-/-</sup> mice and transplanted them with either WT or *Ndufs4*<sup>-/-</sup> bone

✉ e-mail: [yokotat@oici.jp](mailto:yokotat@oici.jp); [brestoff@wustl.edu](mailto:brestoff@wustl.edu)

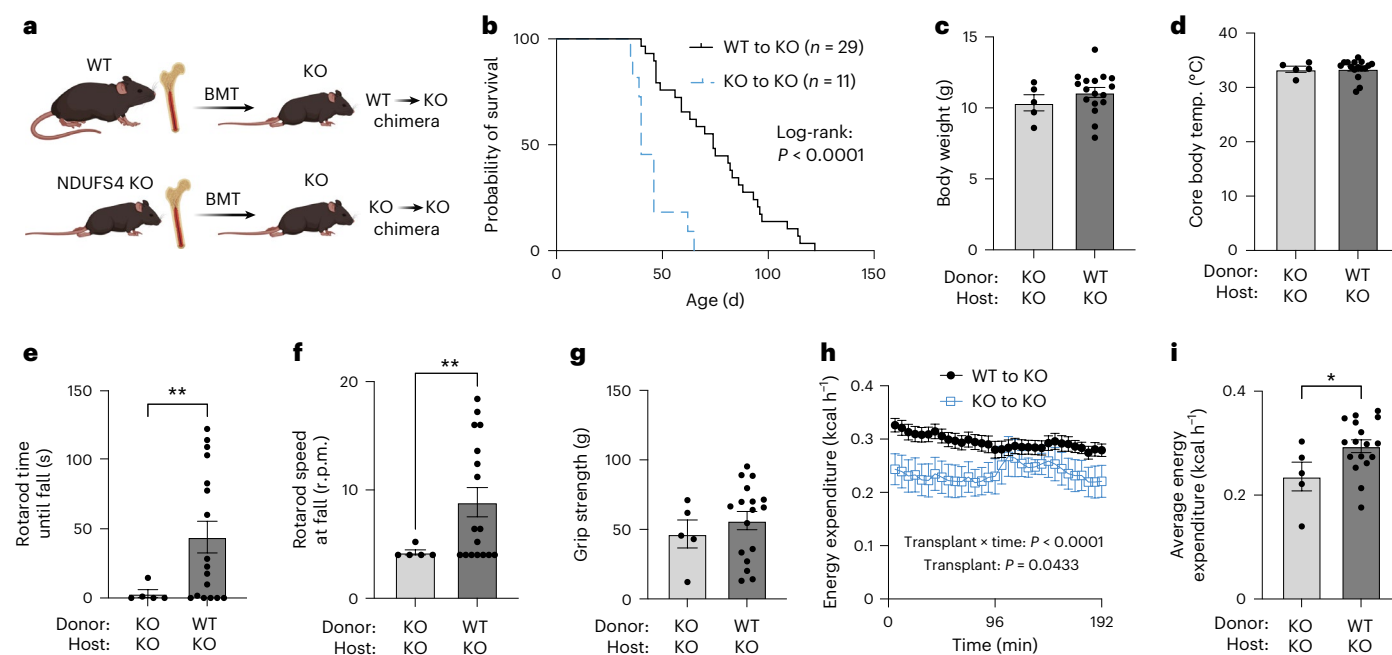


**Fig. 1 | WT BM transplantation (BMT) improves the morbidity and mortality of LS in *Ndufs4*-deficient mice.** **a**, Experimental design. *Ndufs4*<sup>-/-</sup> (KO) mice were lethally irradiated at 3–5 weeks and transplanted with WT or KO BM cells. Created with [BioRender.com](https://BioRender.com). **b**, Survival expressed as postnatal age in days. Solid black line is WT to KO; dashed blue line is KO to KO. **c–g**, Body weight (**c**), rectal core body temperature (**d**), time until falling off a rotarod (**e**), rotarod rotations per minute (r.p.m.) at the time of falling (starting at r.p.m. = 4) (**f**) and four-limb

grip strength at age 7 weeks (**g**). **h**, Energy expenditure shown per interval. Closed black circles are WT to KO; open blue squares are KO to KO. **i**, Average energy expenditure. Data are expressed as the mean ± s.e.m. All data points are unique biological replicates, and all statistical tests are two-sided. For **b**,  $n = 29$  WT to KO,  $n = 11$  KO to KO. For **c–i**,  $n = 5$  KO to WT,  $n = 17$  WT to WT. For **b**, Mantel–Cox log-rank test. For **e**, **f** and **i**, Student's *t*-tests. For **h**, two-way analysis of variance (ANOVA) with repeated measures. \* $P < 0.05$ , \*\* $P < 0.01$ .

marrow (BM; Fig. 1a). We found that WT BM transplantation significantly extended the lifespan of *Ndufs4*<sup>-/-</sup> mice (WT to knockout (KO),  $n = 29$ , median survival of 74 days) compared to *Ndufs4*<sup>-/-</sup> BM transplantation (KO to KO,  $n = 11$ , median survival of 40 days; Mantel–Cox log-rank:  $P < 0.0001$ ; Fig. 1b). Disease severity was assessed 2–4 weeks after transplantation at the age of ~7 weeks, a time point at which peripheral blood donor chimerism was on average  $91.9\% \pm 2.9\%$  (mean ± s.e.m.). Although there were subtle, non-significant improvements in body weight (Fig. 1c) and core body temperature (Fig. 1d), we observed significantly improved performance on a neurological function test where mice are placed on a rotating rod (rotarod). Specifically, KO to KO mice could not maintain balance and fell off the rotarod almost immediately, whereas the majority of WT to KO mice were able to remain on the rotarod for ~1 min on average (Fig. 1e) and tolerate faster rotational speeds (Fig. 1f). Four-limb grip strength did not differ between the mice (Fig. 1g). Next, mice were singly housed in metabolic cages equipped with an activity monitoring system and indirect calorimetry for ~3 h after air equilibration. Whole-body energy expenditure was substantially increased in WT to KO mice compared to KO to KO controls (Fig. 1h,i). The distance travelled exploring this new cage environment was notably higher in some WT to KO mice, but this comparison did not reach statistical significance (Extended Data Fig. 1a). Food pellets and hydrogel were added to the cage bedding to ensure access to food and water during the experiment, making assessments of food and water intake unreliable; therefore, we did not monitor these parameters. However, respiratory exchange ratio (RER), an indicator of energy substrate utilization, did not differ between groups (Extended Data Fig. 1b). Collectively, these data indicate that BM transplantation from healthy, WT donors is associated with improved morbidity and mortality in a mouse model of LS.

To test whether the transplanted haematopoietic cells release mitochondria that are transferred to diseased host cells, we transplanted CD45.1 WT or CD45.1 mtD2<sup>+</sup> BM into lethally irradiated *Ndufs4*<sup>-/-</sup> mice

that naturally have the CD45.2 allele (Fig. 2a). mtD2 is a nuclear-encoded Dendra2 fluorescent protein attached to the mitochondria targeting sequence of cytochrome c oxidase subunit VIII<sup>21</sup> and is a well-established mitochondrial reporter system that enables detection of mitochondria transfer by flow cytometric analyses<sup>4,22</sup>. First, we verified successful engraftment of CD45.1 WT and CD45.1 mtD2<sup>+</sup> immune cells by flow cytometry of peripheral blood 2 weeks after transplantation (Fig. 2b and Extended Data Fig. 2a), and found similar degrees of chimerism between the two groups (Extended Data Fig. 2b). Next, we used small-particle flow cytometry to quantify extracellular mtD2<sup>+</sup> mitochondria in blood, as we described previously using submicron-size calibration beads and antibodies against CD41, TER-119 and CD45 to exclude platelets, red blood cells and immune cell fragments, respectively<sup>4</sup>. We observed that 3.9% (s.e.m. 1.6%) of the submicron particles were mtD2<sup>+</sup> in mtD2 to KO mice compared to 0.0% (s.e.m. 0.0%) in the WT to KO controls (Fig. 2c and Extended Data Fig. 2c). Quantitatively, this corresponded to  $\sim 3.5 \times 10^5$  extracellular mitochondria per ml of blood (Fig. 2d). These results are consistent with prior studies indicating that there are extracellular mitochondria in the blood of mice and humans<sup>23,24</sup> that can be redistributed systemically to distant organs<sup>4,25</sup>.

Recent studies also indicate that immune cells that infiltrate tissues can also transfer mitochondria to parenchymal cells, including transfer of mitochondria from macrophages to neurons in the dorsal root ganglia<sup>26</sup>. To test whether haematopoietic cells transfer mitochondria to host cells in the setting of BM transplantation, we harvested tissues 5 weeks after transplant and observed that ~15–20% of radioresistant host immune cells were mtD2<sup>+</sup> in blood, spleen and liver (Fig. 2e). Furthermore, nearly 100% of splenic non-immune cells and ~20% of liver non-immune cells were mtD2<sup>+</sup> (Fig. 2f). In the spleen, the vast majority of *Ndufs4*<sup>-/-</sup> host-derived B cells, neutrophils, epithelial cells, endothelial cells and stromal cells were mtD2<sup>+</sup>, with significant but lower mtD2<sup>+</sup> frequencies in host T cells and monocytes (Fig. 2g and Extended Data Fig. 3a,b). In the liver, the majority of *Ndufs4*<sup>-/-</sup> host-derived B cells and a

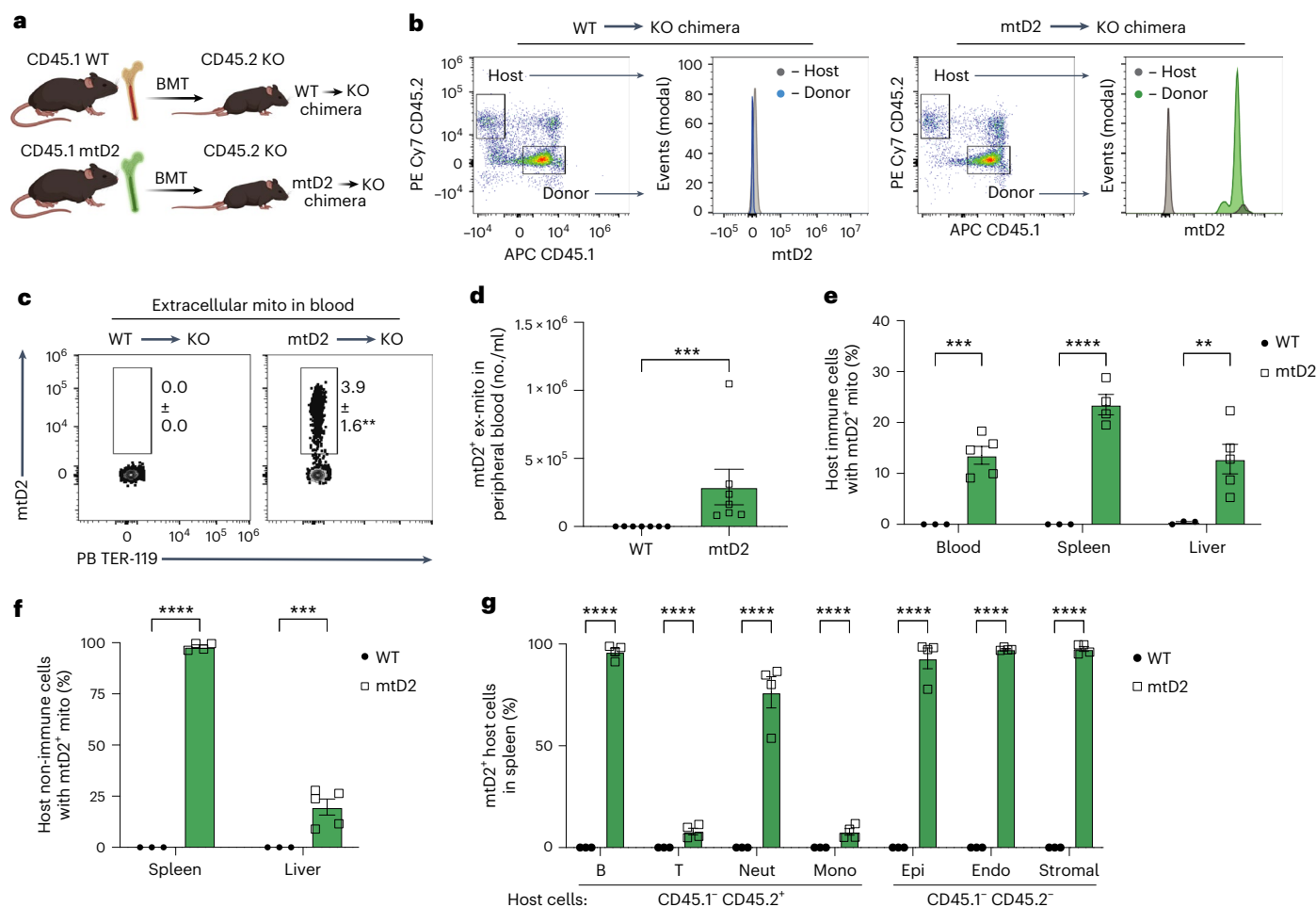


**Fig. 2 | Engrafted haematopoietic cells release mitochondria into the blood and transfer mitochondria to NDUFS4-deficient cells in vivo.** **a**, Experimental design. *Ndufs4*<sup>-/-</sup> (KO) mice were lethally irradiated and transplanted with BM cells from CD45.1 WT or CD45.1 mtD2 mitochondria reporter mice. Created with BioRender.com. **b**, Flow cytometric identification of CD45.1<sup>+</sup> CD45.2<sup>+</sup> donor immune cells and CD45.1<sup>+</sup> CD45.2<sup>+</sup> radioresistant host immune cells. Histograms show mtD2 signal in the host and donor cells within each group. **c**, Flow cytometry plots of extracellular mtD2<sup>+</sup> mitochondria in peripheral blood. Pre-gated on CD41<sup>+</sup> CD45<sup>-</sup> TER-119<sup>-</sup> events less than 2 μm in diameter. **d**, Numbers of mtD2<sup>+</sup> extracellular mitochondria (ex-mito) per ml of peripheral blood. **e, f**, Proportions of singlet, live, CD45.1<sup>+</sup> CD45.2<sup>+</sup> radioresistant host immune cells

(**e**) and CD45.1<sup>+</sup> CD45.2<sup>+</sup> host non-immune cells (**f**) that received mtD2 signal from donor cells in the indicated tissues. **g**, Proportions of host B cells (B), T cells (T), neutrophils (Neut), monocytes (Mono), epithelial cells (Epi), endothelial cells (Endo) and stromal cells that received mtD2 signal from donor cells in the spleen. For **d–g**, closed circles are WT, and open squares are mtD2. Data are expressed as the mean ± s.e.m. All data points are unique biological replicates, and all statistical tests are two sided. For **c** and **d**,  $n = 7$  per group. For **e–g**,  $n = 3$  WT,  $n = 5$  mtD2 (except  $n = 4$  for spleen). For **c** and **d**, Mann–Whitney test. For **e–g**, two-way ANOVA with Sidak post hoc test. \*\* $P < 0.01$ , \*\*\* $P < 0.001$ , \*\*\*\* $P < 0.0001$ . BMT, BM transplantation.

substantial proportion of epithelial, endothelial and stromal cells were mtD2<sup>+</sup>, with lower frequencies of T cells, neutrophils and monocytes that were mtD2<sup>+</sup> (Extended Data Fig. 3c). In the blood, nearly all of the *Ndufs4*<sup>-/-</sup> host-derived B cells and neutrophils were mtD2<sup>+</sup>, with a minor fraction of T cells and monocytes being mtD2<sup>+</sup> (Extended Data Fig. 3d). These data indicate that donor-derived haematopoietic cells provide a source of healthy, cell-free mitochondria, and that BM transplantation is associated with mitochondria transfer to diseased cells in *Ndufs4*<sup>-/-</sup> mice with tissue-specific patterns.

Next, we sought to determine whether inducing mitochondria transfer in the absence of BM transplantation was associated with improved morbidity and mortality in *Ndufs4*<sup>-/-</sup> mice. To accomplish this, we isolated mitochondria from mtD2 mouse livers and confirmed high enrichment of mtD2<sup>+</sup> mitochondria (94.9% ± 1.9%; Extended Data Fig. 4a) and substantially higher yields from liver compared to BM (Extended Data Fig. 4b). Based on this higher yield and much faster isolation of mitochondria from liver than BM, we administered 100 μg liver mitochondria or phosphate-buffered saline (PBS) by intraperitoneal injection 1–2 times per week to *Ndufs4*<sup>-/-</sup> mice. Notably, treatment with

purified mitochondria increased the survival of *Ndufs4*<sup>-/-</sup> mice (Fig. 3a), with median survival of 68 days or 84 days for mice treated with PBS or mitochondria, respectively (Mantel–Cox log-rank:  $P = 0.0052$ ). Body weight (Extended Data Fig. 5a) and core body temperature (Extended Data Fig. 5b) did not differ between groups, and in many but not all instances the mice treated with purified mitochondria rapidly regrew their fur coats (Fig. 3b and Supplementary Video 1). Mice treated with purified mitochondria also exhibited improved balance on a stationary rotarod (Fig. 3c) and a ~20% increase in grip strength (Fig. 3d). Metabolic cage analyses revealed increased energy expenditure in *Ndufs4*<sup>-/-</sup> mice treated with purified mitochondria (Fig. 3e and Extended Data Fig. 5c), whereas distance travelled during the 3-h period did not differ between groups (Extended Data Fig. 5d). RER values did not significantly differ in mitochondria-treated mice, suggesting there was no change in energy substrate utilization (Extended Data Fig. 5e). These data indicate that mitochondria transplantation improves the morbidity and mortality of mice with LS-like disease.

We previously showed that exogenous mitochondria can rescue cell-intrinsic defects in aerobic respiration in macrophages and BV2

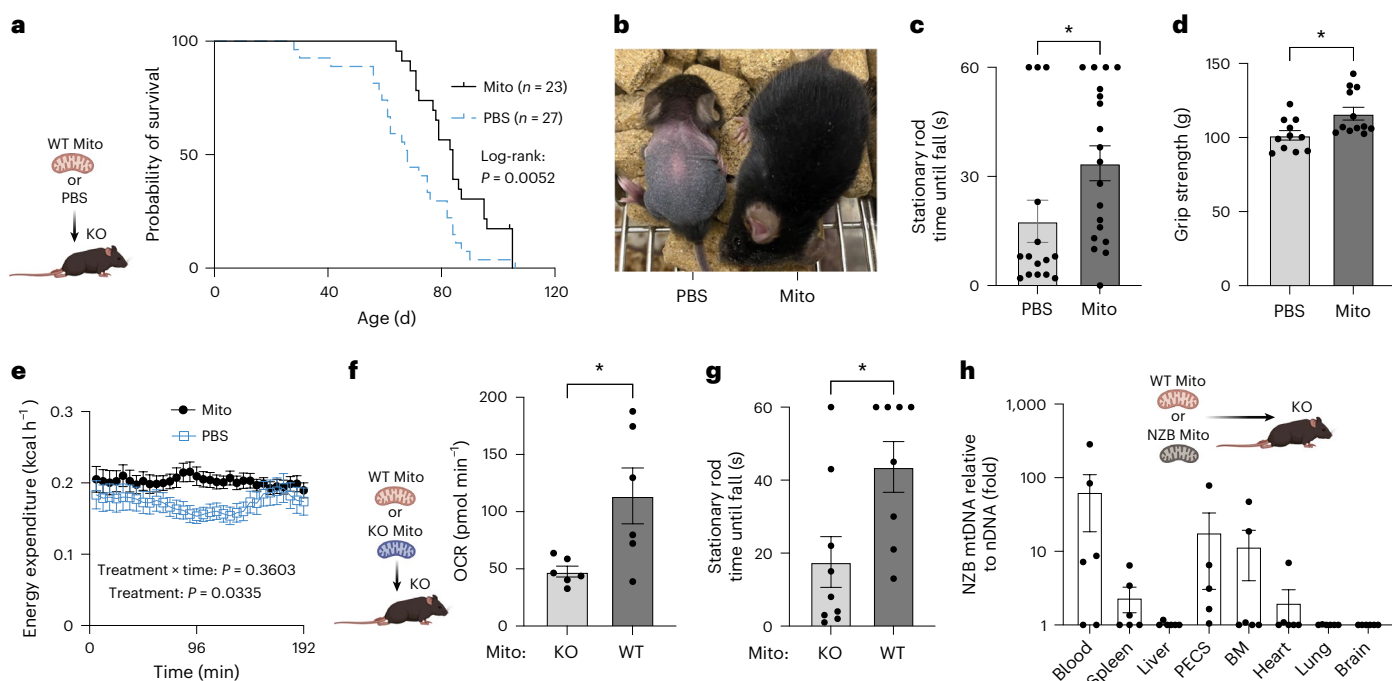


**Fig. 3 | Administration of exogenous mouse mitochondria reduces the morbidity and mortality of LS.** **a**, Experimental design for **a–e**. Survival expressed as postnatal age in days of *Ndufs4*<sup>-/-</sup> (KO) mice treated 1–2 times per week with PBS (dashed blue line) or 100 µg WT mitochondria (Mito, solid black line). Created with [BioRender.com](https://www.biorender.com). **b–e**, Pictures of mice (**b**), time until falling off a stationary rotarod (**c**), four-limb grip strength (**d**) and energy expenditure at 6–8 weeks of age (**e**). **f**, Basal oxygen consumption rate (OCR) of isolated KO or WT mitochondria. Created with [BioRender.com](https://www.biorender.com). **g**, Time until falling off a stationary rotarod by KO mice treated once a week with 100 µg KO or WT mitochondria for 4 weeks. **h**, Tissue biodistribution of NZB mtDNA in

*Ndufs4*<sup>-/-</sup> (KO) mice treated once a week with 100 µg NZB mitochondria for 4 weeks. Background amplification was corrected for with KO mice treated with 100 µg C57BL6/J mitochondria for 4 weeks. Samples were normalized to  $\beta$ -actin as a nDNA control. Created with [BioRender.com](https://www.biorender.com). Data are expressed as the mean  $\pm$  s.e.m. All data points are unique biological replicates, and all statistical tests are two sided. For **c**,  $n = 15$  PBS,  $n = 19$  mito. For **d**,  $n = 11$  PBS,  $n = 12$  mito. For **e**,  $n = 15$  per group. For **d** and **e**, variation in  $n$  is due to mortality kinetics. For **f**,  $n = 6$  per group. For **g**,  $n = 9$  KO mitochondria,  $n = 8$  WT mitochondria. For **h**,  $n = 6$  per tissue. For **a**, Mantel–Cox log-rank test. For **c**, **d**, **f** and **g**, Student's *t*-tests. For **e**, Mann–Whitney test. \* $P < 0.05$ .

cells, and this response is dependent on expression of NDUFS4 by the donor mitochondria<sup>4</sup>. To test whether mitochondria transplantation ameliorates LS in an NDUFS4-dependent manner, we isolated WT or *Ndufs4*<sup>-/-</sup> liver mitochondria for administration to *Ndufs4*<sup>-/-</sup> mice. The oxidative consumption rate was significantly lower in isolated mitochondria obtained from *Ndufs4*<sup>-/-</sup> livers compared to WT controls (Fig. 3f), demonstrating severe impairment of oxidative phosphorylation. Notably, 6 weeks of weekly intraperitoneal injection with 100 µg WT but not *Ndufs4*<sup>-/-</sup> mitochondria improved balance on a stationary rod (Fig. 3g). These data indicate that the therapeutic benefit of mitochondria transplantation in LS is dependent on NDUFS4, suggesting that bioenergetic effects might partially contribute to the observed improvement in neurological function.

To determine the tissue biodistribution of the transplanted mitochondria, we used isolated mitochondria from the livers of C57BL6/J or NZB/BINJ (NZB) mice, which have a mitochondrial DNA (mtDNA) genome that has >76 polymorphisms compared to the C57BL6/J reference mtDNA genome and that can be detected using amplification refractory mutation system (ARMS)-PCR<sup>27</sup>. This approach was used instead of mtD2-labelled mitochondria because the mtDNA genome can be maintained in recipient cells, whereas the mtD2 protein cannot. We administered 100 µg of C57BL6/J or NZB mitochondria by intraperitoneal injection once per week to *Ndufs4*<sup>-/-</sup> mice for 5 weeks and then harvested various tissues, with peritoneal exudate cells (PECS) serving as a positive control. We observed NZB mtDNA in the PECS, blood, spleen and BM, whereas the signal was below the limit of detection in the liver, lung, heart and brain (Fig. 3h). These analyses were normalized to  $\beta$ -actin nDNA content to account for cellularity in the tissue biopsy samples. These results suggest that the mtDNA from

mitochondria transplanted via intraperitoneal injection is distributed in lymphoid-related tissues.

Several studies indicate that uptake of healthy extracellular mitochondria by immune cells such as macrophages and T cells has anti-inflammatory effects<sup>28–31</sup>. Indeed, it was recently reported that inflammation contributes to LS disease pathogenesis<sup>32–34</sup>. Therefore, we hypothesized that mitochondria transplantation might attenuate inflammation in *Ndufs4*<sup>-/-</sup> mice. To assess this possibility, we first compared the peripheral blood immune cell composition in *Ndufs4*<sup>-/-</sup> mice treated with PBS or 100 µg WT mitochondria weekly for 5 weeks (Extended Data Fig. 6a). We found that there were no changes in the numbers per millilitre of B cells, eosinophils, natural killer (NK) cells, neutrophils, monocytes, CD4<sup>+</sup> T cells or CD8<sup>+</sup> T cells between the two groups (Extended Data Fig. 6b). Second, we treated *Ndufs4*<sup>-/-</sup> mice with WT or KO mitochondria for 6 weeks and observed no differences in the numbers of these seven immune cell populations in the blood (Extended Data Fig. 7a), spleen (Extended Data Fig. 7b), BM (Extended Data Fig. 7c) or liver (Extended Data Fig. 7d). Third, we compared the expression of inflammatory cytokines in the spleen (Extended Data Fig. 8a), PECS (Extended Data Fig. 8b) and liver (Extended Data Fig. 8c), and found that the relative expression of interleukin (IL)-6, tumour necrosis factor (TNF), interferon (IFN)- $\gamma$ , IL-18 and IL-4 did not differ in *Ndufs4*<sup>-/-</sup> mice treated with WT or KO mitochondria weekly for 6 weeks. These data suggest that weekly administration of isolated mitochondria to *Ndufs4*<sup>-/-</sup> mice does not attenuate or enhance inflammation in these organs, although we cannot formally exclude a potential effect of mitochondria transplantation on inflammatory responses.

It is known that human mitochondria can fuse with endogenous mitochondria in mouse cells, although human proteins are not

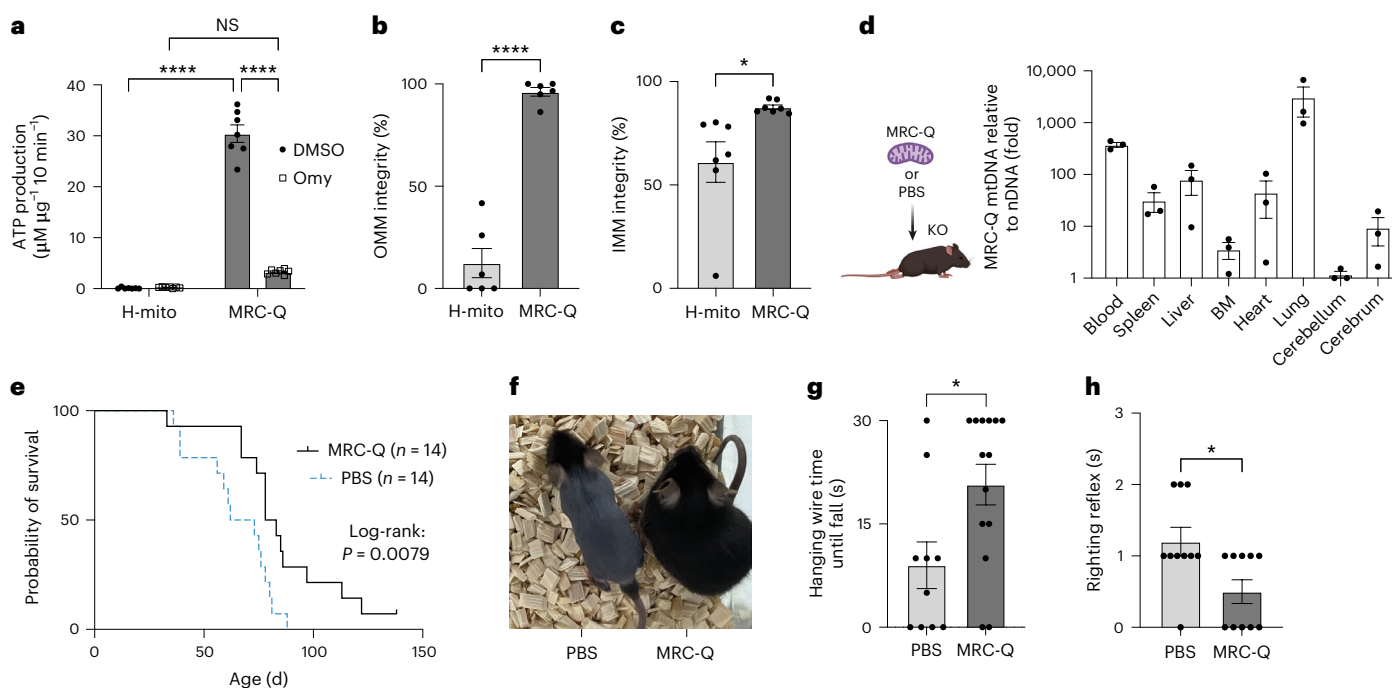


**Fig. 4 | Administering a human mitochondria isolate called MRC-Q improves the morbidity and mortality of LS.** **a**, Production of ATP in the presence of dimethylsulfoxide (DMSO) or oligomycin (Omy) by mitochondria isolated from HeLa cells by a commercial kit (H-mito) or MRC-Q. **b,c**, Outer mitochondrial membrane (OMM) (**b**) and inner mitochondrial membrane (IMM) (**c**) integrity. **d**, Tissue biodistribution of MRC-Q mtDNA in *Ndufs4*<sup>-/-</sup> (KO) mice treated with 50 µg MRC-Q once per week for 4 weeks. Background amplification was corrected for with KO mice treated with PBS for 4 weeks. Samples were normalized to β-actin as a nDNA control. Created with [BioRender.com](https://BioRender.com). **e**, Survival

expressed as postnatal age in days. MRC-Q, solid black line. PBS, dashed blue line. **f–h**, Pictures of mice (**f**), time until falling off a hanging wire at age 7 weeks old (**g**) and righting reflex delay when mice were placed on their backs (**h**). Data are expressed as the mean ± s.e.m. All data points are unique biological replicates, and all statistical testing is two sided. For **a** and **d**, *n* = 7 per group. For **c**, *n* = 6 per group. For **d**, *n* = 3 per tissue. For **g**, *n* = 10 PBS, *n* = 14 MRC-Q. For **h**, *n* = 10 per group. For **a**, two-way ANOVA. For **b, c, g** and **h**, Student's *t*-tests. For **e**, Mantel–Cox log-rank test. \**P* < 0.05, \*\*\*\**P* < 0.0001. NS, not significant.

maintained over longer periods of time<sup>35</sup>. Therefore, in a translational effort, we tested whether xenogenic transplantation of human mitochondria is associated with increased survival in *Ndufs4*<sup>-/-</sup> mice. We obtained HeLa cell-derived human mitochondria organelle complex-Q (MRC-Q; LUCA Science), a cell-free product enriched in mitochondria that can be frozen to support distribution and storage and then thawed before administration. Compared to human mitochondria isolated from the same cellular source with traditional homogenization and differential centrifugation enrichment methods (H-mito), thawed MRC-Q exhibited higher ATP production that was suppressed after adding the ATP synthase inhibitor oligomycin (Fig. 4a) and had substantially better integrity of the outer mitochondrial membrane (Fig. 4b) and inner mitochondrial membrane (Fig. 4c). These data indicate that freeze-thawed MRC-Q is highly enriched in intact mitochondria that retain their ability to respire. We administered 50 µg MRC-Q to 3-week-old *Ndufs4*<sup>-/-</sup> mice intravenously once per week for 4 weeks and observed human mtDNA in various organs including in the blood, spleen, liver, BM, heart, lung and brain after perfusion with PBS, with the highest signal observed in the lung (Fig. 4d). Each sample was normalized to mouse nDNA content to account for cellularity.

Next, we treated *Ndufs4*<sup>-/-</sup> mice with PBS or MRC-Q intravenously and found that MRC-Q treatment significantly improved the survival of *Ndufs4*<sup>-/-</sup> mice (median survival 80.5 days) compared to PBS-treated controls (median survival 67.5 days, Mantel–Cox log-rank: *P* = 0.0079; Fig. 4e). Body weights did not differ between groups (Extended Data Fig. 9); however, MRC-Q-treated mice frequently regrew their fur (Fig. 4f), exhibited increased capacity to hang onto a wire (Fig. 4g) and had a faster righting reflex (Fig. 4h and Supplementary Video 2) compared to PBS-treated controls. MRC-Q-treated mice also had improved stability and posture when suspended by the tail and landed on four

limbs when released from low height to the cage bedding (Supplementary Video 3). In contrast, PBS-treated mice gyrated unstably during tail suspension and landed on their backs after release to the cage bedding (Supplementary Video 3). These data suggest that intravenous MRC-Q human mitochondria are distributed to various tissues and ameliorate the morbidity and mortality of *Ndufs4*<sup>-/-</sup> mice.

These studies reveal that mitochondria transfer pathways can be harnessed therapeutically to treat inherited mitochondrial diseases, such as LS. First, transplantation of WT BM to *NDUFS4*-deficient mice ameliorates LS and is associated with delivery of donor cell-derived mitochondria to diseased host cells. Second, mitochondria transplantation recapitulates many of the beneficial outcomes observed following WT BM transplantation. A comparison of the three therapeutic paradigms is provided in Extended Data Table 1. We reported true survival; therefore, our control groups have longer median survival than other studies that utilize euthanasia criteria<sup>32,36</sup>. True survival was determined because some euthanasia criteria are subjective and/or transient (for example immobility) or do not reflect future lifespan accurately (for example, low core body temperature).

The mechanisms by which mitochondria transfer-related therapies ameliorate LS are unclear. Although this study does not provide direct evidence that the uptake of donor mitochondria alters the bioenergetics of acceptor cells in vivo, we speculate that a bioenergetic mechanism is plausible. This possibility is supported by four lines of evidence. First, transplantation of mitochondria from WT but not *Ndufs4*<sup>-/-</sup> mice ameliorated LS in our studies. Second, healthy mitochondria can be taken up and utilized to rescue cell-intrinsic defects in aerobic respiration in *Ndufs4*<sup>-/-</sup> peritoneal macrophages in vivo and in *p*<sup>0</sup> cells that lack mtDNA in vitro<sup>4–7</sup>. Third, BV2 cells exposed to a brief pulse of rotenone and antimycin A had impaired aerobic

respiration that could be rescued by uptake of WT but not *Ndufs4*<sup>-/-</sup> mitochondria<sup>4</sup>. Fourth, complex I regenerates NAD<sup>+</sup> during oxidative phosphorylation and is critical for ATP production. It is possible that delivery of NAD<sup>+</sup>, ATP, or other mitochondrial metabolites ameliorates LS. Indeed, prior studies showed that administering NAD<sup>+</sup> precursors (for example, nicotinamide mononucleotide) or expressing the yeast NADH dehydrogenase NDII to restore NAD<sup>+</sup> synthesis decreases LS disease severity in *Ndufs4*<sup>-/-</sup> mice<sup>37,38</sup>.

The *Ndufs4*<sup>-/-</sup> mouse develops prominent central nervous system dysfunction, and we demonstrate using rotarod assays that neurological function is improved following BM or mitochondria transplantation. However, our tissue biodistribution studies revealed no, or at best very little, donor-derived mtDNA in the brains of *Ndufs4*<sup>-/-</sup> mice. This is a puzzling result and raises additional questions about how neurological function and survival could be improved in this context. One possibility is that the exogenous mitochondria might be taken up by cells in the peripheral nervous system, including peripheral neurons, which would not be detected in our flow cytometric assays. This could potentially improve peripheral neuropathy or reflex dysfunction that occurs in LS<sup>39</sup>. Indeed, we observed that mitochondria transplantation improved the righting reflex of *Ndufs4*<sup>-/-</sup> mice. A second possibility is that the exogenous mitochondria may induce expression of antioxidant enzymes that quench reactive oxygen species and limit accumulation of oxidative stress-associated cellular damage in diseased cells, a process that was shown to occur in the heart<sup>25</sup>. Third, recent studies demonstrate that transplanted mitochondria elicit mitophagy<sup>16</sup>, raising the possibility that mitochondria transfer-related therapies ameliorate LS by enhancing mitophagy to reduce or delay the accumulation of damaged mitochondria. These potential mechanisms for how mitochondria transfer-based therapies ameliorate LS should be explored in future studies.

There are several limitations of this study. Notably, the tissue biodistribution studies of donor mtDNA were normalized to mouse nDNA content to account for cellularity. We did not determine the percentage of total mtDNA that was derived from donor mitochondria because (1) all cells in tissues have mtDNA but not all of those cells take up donor-derived mitochondria, (2) some cell types take up mitochondria much more efficiently than others, and (3) the mtDNA copy number per cell can vary dramatically across tissues. This precludes us from quantifying how much mtDNA or how many mitochondria were taken up in the various tissues, and we have not defined which cell types take up the transplanted mitochondria. Therefore, the exact mechanisms of how transplanted mitochondria improve survival and ameliorate LS severity remain unclear. Future studies are needed to determine the cellular distribution of transplanted mitochondria, the bioenergetic effects of mitochondria transfer on individual cell types *in vivo*, and the fate and maintenance of the transplanted mitochondria.

Given the complexity of mitochondria transfer pathways and the cell-type-specific effects of this process, it is likely that mitochondria transfer-based therapies for LS or other diseases will involve multifaceted mechanisms of action. An exciting future direction will be to determine the safety and efficacy of heterologous haematopoietic stem cell or mitochondria transplants in clinical trials for patients with primary mitochondrial diseases, such as LS.

## Methods

### Mice

Experiments performed at Washington University School of Medicine utilized the following mouse strains procured from Jackson Laboratories: WT C57BL6/J (strain no. 000664), CD45.1 (Ptprca, strain number 002014), PhAM<sup>excised</sup> (also known as mtDendra2 or mtD2, strain no. 018397) and *Ndufs4*<sup>+/-</sup> (strain no. 027058) and New Zealand Black (NZB, strain no. 000684). CD45.1 mtD2<sup>+/-</sup> mice were generated by crossing mtD2 mice onto a CD45.1 homozygous background. The other strains are on a CD45.2 background. Experiments performed at Osaka

University (OU) utilized the following mouse strains procured from Clea Japan unless otherwise noted: WT C57BL6/J, *Ndufs4*<sup>+/-</sup> (Jackson Labs via LUCA Science) and CD45.1 (Jackson Labs). All mice were on a C57BL6/J background, except for NZB mice. *Ndufs4*<sup>-/-</sup> mice were generated by crossing heterozygous males and females from Jackson Labs stock as duos (1 female and 1 male) or trios (2 females and 1 male per cage), with timed breeding to generate many litters born within a few days of each other. Heterozygotes from that cross were used for subsequent breeding. All mice were housed in a specific pathogen-free barrier facility at room temperature with a 12-h–12-h light–dark cycle, with lights on at 06:00 and lights off at 18:00, and had access to food and water *ad libitum*. The animal facilities were maintained at room temperature (range of 20–26 °C at WashU, range of 21.5–24.5 °C at OU) with a target humidity setpoint of 30–70% at WashU and 45–65% at OU. Male and female *Ndufs4*<sup>-/-</sup> mice were used interchangeably and in similar proportions with treatment starting at age 3–5 weeks old. True survival was determined as the actual date of death minus the date of birth without using euthanasia criteria. To harvest tissues, separate experiments were performed from survival curve studies, and mice were euthanized using isoflurane asphyxiation before tissue procurement. In some cases, tail vein blood was collected from awake mice. Studies performed at Washington University School of Medicine were approved under Institutional Animal Care and Use Committee protocol no. 22-0286. Studies performed at OU were approved by the Institutional Animal Care and Use Committee at OU Graduate School of Medicine (approval no. 30-096-013).

### BM transplantation

*Ndufs4*<sup>-/-</sup> recipient mice aged 3–5 weeks old were lethally irradiated with 650–800 rads using an X-ray irradiator in a specific pathogen-free barrier facility. Immediately after irradiation, donor BM was isolated from the femurs and tibias from CD45.1 *Ndufs4*<sup>+/+</sup> (WT), CD45.1 *Ndufs4*<sup>+/-</sup> or CD45.1 mtD2<sup>+/-</sup> mice. BM cells were isolated from the marrow cavity by cutting the bone tips and placing them inside sterile 600  $\mu$ l polypropylene tubes (Eppendorf) with a hole poked into the bottom with a 16-gauge needle. The 600- $\mu$ l tube and bones were placed inside sterile 1.5-ml polypropylene tubes (Eppendorf) and centrifuged at 8,000g at 4 °C for 15 s. BM cell collection was verified by observing a red cell pellet and whitened bone shafts. The bones were discarded, and the cells were resuspended in 1 ml ACK RBC Lysis Buffer (Gibco) for 5 min at room temperature to lyse mature red blood cells. The lysis reaction was quenched with 10 ml sterile wash buffer, comprising high-glucose DMEM (Gibco or Corning) supplemented with 5% heat-inactivated FBS, 1 $\times$  penicillin–streptomycin (Gibco) and 2 mM L-glutamine (Gibco). The cells were centrifuged at 500g at 4 °C for 5 min in a swinging-bucket centrifuge (Eppendorf 5810 R), supernatant was aspirated, and the cell pellet was resuspended in 10 ml sterile PBS. The cells were centrifuged again as described above and resuspended in 2–5 ml sterile PBS for cell counting using 1:1 ratios of cells and 0.1% trypan blue in PBS, with live-cell identification using either a Countess FL or a hemacytometer. Cell counts were performed in triplicate. The cells were pelleted by centrifugation, as described above, the supernatants were aspirated, and the cells were resuspended in PBS at a final concentration of 2  $\times$  10<sup>8</sup> cells per ml. Male and female cells were processed separately and transplanted to sex-matched recipients under 1–2% isoflurane anaesthesia by retro-orbital injection at volumes of 50  $\mu$ l (10 million cells per recipient). The mice were returned to their home cage over a warming pad until fully recovered. Water bottles containing 3.3% sulfamethoxazole–trimethoprim oral suspension USP (STM, Aurobindo) were provided for 2 weeks, with remixing every 1–2 days and replacement after 7 days. The STM drinking water was made by adding 8 ml STM oral suspension (200 mg sulfamethoxazole and 40 mg trimethoprim per 5 ml) to a 240-ml bottle of autoclaved mouse water. Engraftment was assessed by collecting 5  $\mu$ l of blood from the tail vein with milking and performing flow cytometric analyses, as described below.

### Murine mitochondria isolation

Murine mitochondria were isolated using the Mitochondria Isolation Kit, Mouse Tissue (Miltenyi Biotec). Briefly, *Ndufs4*<sup>+/+</sup>, *Ndufs4*<sup>-/-</sup> or NZB mice were euthanized and perfused with 10 ml sterile PBS using a peristaltic pump via the heart's left ventricle. Perfused livers were harvested, finely minced and transferred to a 2-ml glass dounce homogenizer. A 1-ml aliquot of ice-cold Lysis Buffer (Miltenyi Biotec) containing 10  $\mu$ l of 100 $\times$  Halt Protease Inhibitor Cocktail (Thermo Fisher) was added, and eight strokes were performed with twisting downward and straight upward movements. The homogenate was transferred to sterile 15-ml conical tubes, and 9 ml of 1 $\times$  Separation Buffer was added. The specimen was mixed by gentle inversion, and then 50  $\mu$ l of anti-TOM20 Microbeads were added. The specimen was wrapped in foil and rocked at 4  $^{\circ}$ C for 60 min. The sample was pulse centrifuged at 500g at 4  $^{\circ}$ C for  $\sim$ 5 s to pellet large debris and then held on ice as the supernatant was passed over an LS column attached to a QuadroMACS magnet with stand. The entire supernatant volume was passed through the column and then washed three times with 2 ml ice-cold 1 $\times$  Separation Buffer. After the third wash, the LS column was removed from the magnet, and the bound mitochondria were eluted into a new 15-ml conical tube using 1.5 ml ice-cold 1 $\times$  Separation Buffer with gentle LS column plunger force to avoid bubbles. The eluted mitochondria were centrifuged at 13,000g at 4  $^{\circ}$ C for 2 min to pellet the mitochondria. Supernatants were discarded and the mitochondria were resuspended in 1–1.5 ml Storage Buffer. Protein concentration was measured using 10  $\mu$ l of the mitochondria isolate and 250  $\mu$ l Coomassie Reagent Plus (Thermo Fisher), with BSA (Pierce) serial dilutions as a standard curve. Mitochondria isolates were aliquoted, centrifuged at 13,000g for 2 min, and brought to concentrations of 500  $\mu$ g ml<sup>-1</sup> in ice-cold PBS. Mice were then treated with 200  $\mu$ l (100  $\mu$ g) of the mitochondria isolates or PBS by intraperitoneal injection.

### Neurological performance testing

Four-limb grip strength was measured using a Bioseb grip-strength meter with a mesh grid (BIO-GS3). Consistent, smooth force was applied using Bioseb Acquisition Software (BIO-CIS version 1.5.1.0(En), Bioseb) guidance, and the maximum force at the time of release was recorded. Mice were placed on stationary rotarods equipped with eight infrared lasers per lane to determine the time at which the mouse fell off. The rotation speed ramped up gradually from 4.0 r.p.m. with a rate of increase of 1.2 r.p.m. per minute. If one group fell off the stationary rod before starting the rotations, the rod was left stationary for the other group. For the hanging wire test, mice were hung from a horizontal rod (1 cm in diameter, at a height of 20 cm) by their forelimbs. After hanging, the time until fall was measured for up to 30 s.

### Metabolic cages

Mice were weighed, and core body temperature was measured using a RET-3 mouse rectal probe and Fluke 51-II handheld thermometer. The mice were then singly housed for 4 h in a 16-cage Comprehensive Laboratory Animal Monitoring System (CLAMS, Columbus Instruments). Energy expenditure and RER were calculated as previously described<sup>22</sup>. The enclosure temperature was set at 22.2  $^{\circ}$ C with a 12-h–12-h light–dark cycle with lights on at 06:00 and lights off at 18:00. Air exchange was equilibrated for 1 h before recording. Food pellets and hydrogel were placed on the bedding because the mice could not reach the hanging feeder or water bottle easily, precluding measurement of food or water intake. Distance travelled was determined using an array of infrared lasers and Oxymax software version 5.66 (Columbus Instruments).

### Flow cytometric detection of extracellular mitochondria in blood

Peripheral blood was sampled from the tail vein, and 5  $\mu$ l blood was transferred to 245  $\mu$ l ACK RBC Lysis Buffer containing 1 mg ml<sup>-1</sup> heparin (grade 1 A, Sigma-Aldrich) with gentle mixing. The cells were pelleted by

centrifugation at 500g at 4  $^{\circ}$ C for 5 min. The cell-free supernatant was collected (200  $\mu$ l, equal to 80% of the total volume) for small-particle flow cytometry to detect extracellular mitochondria in blood, as previously described<sup>4</sup>. In brief, the cell-free fraction was pelleted at 15,000g at 4  $^{\circ}$ C for 5 min, and the supernatant was removed before resuspending the pellet in 50  $\mu$ l staining buffer containing the following antibodies: BV421-CD41 (MWRReg30, BioLegend; 1:300 dilution), PB-TER-119 (TER-119, BioLegend; 1:300 dilution) and PerCP/Cy5.5-CD45 (30-F11, BioLegend; 1:200 dilution). The particles were washed by adding 1 ml FACS buffer (PBS containing 2.5% heat-inactivated FBS and 2.5 mM EDTA followed by filter-sterilization) and centrifuging the samples at 15,000g at 4  $^{\circ}$ C for 5 min. The pelleted particles were resuspended in a final volume of 200  $\mu$ l FACS buffer, and flow cytometry was performed on a four-laser Cytek (16V-14B-10YG-8R configuration using SpectroFlo v2.0 software) with small-particle settings (FSC = 675, SSC = 235–255, threshold = 6,000). Submicron-size calibration beads loaded with FITC (Thermo Fisher) were used to identify particles under 2  $\mu$ m and to set gains to detect the smallest possible particles, with a 300-nm lower limit of detection for this cytometer. We then acquired 100  $\mu$ l of each specimen. Extracellular mitochondria were defined as CD45<sup>-</sup> CD41<sup>+</sup> TER-119<sup>+</sup> particles <2  $\mu$ m in diameter and mtD2<sup>+</sup>. Mitochondria percentages were defined as the percentage of all CD45<sup>-</sup> CD41<sup>+</sup> TER-119<sup>+</sup> particles that were mtD2<sup>+</sup>. Cell-free mitochondria counts in 1 ml of blood were defined as total mtD2<sup>+</sup> events  $\times$  2 (to account for acquiring half the stained specimen)  $\times$  1.25 (to account for processing 80% of the original specimen's volume)  $\times$  200 (to account for collecting 5  $\mu$ l of whole blood).

### Flow cytometric analyses of cells

In some cases, peripheral blood from the tail vein was collected, as described in the section on flow cytometric detection of cell-free mitochondria in blood; however, pelleted cells were collected for processing. Mice were perfused with 10 ml PBS, as described above, and the spleens and livers were dissected. Spleen cells were obtained by mashing them through a 100- $\mu$ m strainer using a sterile syringe plunger and washed with Wash Media. To isolate cells from the BM, the soft tissue was removed from one femur and tibia, and BM cells were isolated using the centrifugation method described above. The pelleted BM was resuspended in Wash Media. Liver non-parenchymal cells were isolated by finely mincing the livers using a razor blade and processed according to established protocols<sup>40</sup>. Briefly, minced livers were digested in high-glucose DMEM containing 0.75 mg ml<sup>-1</sup> collagenase A (Sigma) and 50  $\mu$ g ml<sup>-1</sup> DNase I (Sigma) for 30 min in an orbital shaker at 140 r.p.m. at 37  $^{\circ}$ C. Liver digests were centrifuged at 50g at 4  $^{\circ}$ C for 3 min to pellet hepatocytes. Supernatant containing non-parenchymal cells was carefully pipetted into a fresh conical tube. Spleen, liver non-parenchymal and BM cells were resuspended in 1–2 ml ACK RBC Lysis Buffer and incubated at room temperature for 5 min. The reaction was quenched by adding 10 ml Wash Media. The cells were pelleted and collected in 96-well round-bottom plates for staining. The cells from blood, spleen, liver and/or BM were spun in a swinging-bucket centrifuge at 500g at 4  $^{\circ}$ C for 5 min, and the supernatants were flicked off. Cells were washed once in 200  $\mu$ l PBS, followed by immediate centrifugation at 500g at 4  $^{\circ}$ C for 3 min. The supernatants were discarded, and the cells were resuspended in 50  $\mu$ l PBS containing Zombie NIR viability dye (1:1,000 dilution in PBS, BioLegend) and incubated on ice for 5 min. The reaction was quenched by adding 200  $\mu$ l FACS buffer. The cells were pelleted at 500g at 4  $^{\circ}$ C for 5 min, and then resuspended in 25  $\mu$ l Mouse BD Fc Block (anti-CD16/32, BD Pharmingen) at 1:100, diluted in FACS buffer. After 15 min on ice, a 25- $\mu$ l aliquot of a 2 $\times$  antibody cocktail in Brilliant Stain Buffer (BD) was added to the cells and mixed by gently pipetting up and down. The cells were stained with PE/Cy7-CD45.2 (clone 104, BioLegend; 1:200 dilution) and APC-CD45.1 (clone A20, BioLegend; 1:200 dilution) to identify donor and host immune cells. Immune cell populations were

further characterized with the following antibodies: PerCP-CD45 (30-F11, BioLegend; 1:200 dilution), BV421-SiglecF (E50-2440, BD; 1:400 dilution), Spark-NIR685-CD19 (6D5, BioLegend; 1:300 dilution), BV750-B220 (RA3-6B2, BioLegend; 1:300 dilution), APC/Fire810-NK1.1 (S17016D, BioLegend; 1:300 dilution), AF488-TCR $\beta$  (H57-597, BioLegend; 1:300 dilution), PE/Fire640-CD4 (GK1.5, BioLegend; 1:300 dilution), SB550-CD8 (53-6.7, BioLegend; 1:300 dilution), PB-CD11b (M1/70, BioLegend; 1:400 dilution), BV711-Ly6G (1A8, BioLegend; 1:300 dilution) and AF700-Ly6C (HK1.4, BioLegend; 1:300 dilution). Cells were stained for 30 min on ice and then washed twice with 200  $\mu$ l FACS buffer before final resuspension in a volume of 200  $\mu$ l. For each specimen, 100  $\mu$ l cell suspension was acquired on a Cytex Aurora (SpectroFlo v2.0 software). Analyses of flow cytometry data were conducted with FlowJo (BD) version 10.8 or 10.9 software.

### Seahorse assay

Mitochondria were isolated from the livers of WT or *Ndufs4*<sup>-/-</sup> mice and 50  $\mu$ g of mitochondria was plated onto eight-well Agilent Seahorse XF HS PDL Miniplates (Agilent Technologies). Mitochondria were centrifuged at 2,000g for 20 min at 4 °C and mitochondria seahorse assay media (1 mM pyruvate, 2 mM glutamine, 10 mM glucose, 70 mM sucrose, 18 mM EDTA and 0.2% wt/vol BSA in Seahorse media) was added to each well. Mitochondrial basal oxygen consumption rate was measured using an Agilent Seahorse XFp HS Mini machine with software version 3.0.0.25.

### MRC-Q reagent collection, preparation and administration

MRC-Q was isolated from HeLa cells (JCRB Cell Bank, cell no. JCRB9004) by iMIT (WO2021015298). Briefly, cultured cells with greater than 90% confluency were treated with 30  $\mu$ M digitonin (WAKO, 043-21376) for 3 min on ice. Cells were washed twice with Tris-sucrose buffer (10 mM Tris (WAKO, 011-20095)/250 mM sucrose (WAKO, 193-09545)/0.5 mM EGTA (DOJINDO, 348-01311), pH 7.4) and incubated in Tris-sucrose buffer for 10 min on ice. Cells were detached by gentle pipetting for 3 min and cell suspensions were collected into an ice-cold test tube. Cell debris was removed by two rounds of centrifugation at 500g for 10 min at 4 °C. Supernatant containing mitochondria and other organelles was collected and centrifuged at 3,000g for 10 min at 4 °C. Pelleted mitochondria were resuspended in Tris-sucrose buffer and quantified by Pierce 660 nm Protein Assay Kit (Thermo, 22662). The mitochondria solution (MRC-Q) was diluted further in Tris-sucrose buffer if necessary and stored at -80 °C. Isolation of mitochondria with a traditional homogenized method (H-mito) was conducted with the Mitochondrial Isolation Kit (Thermo, 89874). Cell cultures of over 80% confluency were transferred to a 1 ml dounce homogenizer (DURAN WHEATON KIMBLE, 357538) and homogenized with 60 strokes of the plunger before proceeding to processing and storage as described for MRC-Q. MRC-Q was cryopreserved at -80 °C and then thawed before use. MRC-Q was cryopreserved at a concentration of 100  $\mu$ g per 100  $\mu$ l in 10 mM Tris-sucrose (250 mM) plus EGTA (0.5 mM), thawed in a constant temperature bath at 25 °C for about 2 min and stored on ice. After centrifugation at 3,000g for 15 min (slow acceleration and slow brake), the supernatant was removed and diluted with PBS to a concentration of 50  $\mu$ g per 60  $\mu$ l. *Ndufs4*<sup>-/-</sup> mice were injected with MRC-Q intravenously through the orbital venous plexus under anaesthesia. The MRC-Q group received 50  $\mu$ g of MRC-Q resuspended in 60  $\mu$ l of PBS per mouse, once a week starting at 3 weeks old and ending at 7 weeks old. The control group received 60  $\mu$ l PBS per mouse in the same manner as mice in the MRC-Q group.

### Mitochondrial ATP production assay

The amount of ATP produced by MRC-Q and H-mito was evaluated using the luciferin-luciferase bioluminescence reaction. ATP production reaction was performed for 10 min at room temperature in 50  $\mu$ l reaction volume, in a half-area 96-well plate. The reaction

mixture included: 10 mM malate (WAKO, 199-05642), 5 mM glutamate (WAKO, 194-02032), 10 mM KH<sub>2</sub>PO<sub>4</sub> (WAKO, 164-04245), 0.1 mM ADP (Sigma-Aldrich, A2754-1G), 70 mM KCl (WAKO, 163-03545) with or without 5  $\mu$ M oligomycin A (Selleckchem, S1478). Isolated mitochondria (0.5  $\mu$ g protein) were added to each well. To quantify the amount of ATP produced, the ATP standard solution was diluted with Tris buffer (10 mM Tris-HCl, 250 mM sucrose, 0.5 mM EGTA, pH 7.4) to 0.1, 0.3, 1, 3, 10 or 30  $\mu$ l and added to each well. The reaction was stopped by 10-min incubation on ice, after which 50  $\mu$ l of luciferase reagent (Cell Titer-Glo, Promega) was added. The mixture was incubated at 37 °C for 2 min and equilibrated to room temperature for 10 min before luminescence was measured with a plate reader (Spark, Tecan). The amount of ATP produced was calculated from the emission intensities of the obtained standard curve and samples.

### Measurement of inner membrane integrity and outer membrane integrity of isolated mitochondria

Inner membrane integrity was spectrophotometrically determined by formation of 2-nitro-5-benzoic acid from 5,5'-dithiobis(2-nitrobenzoic acid) and CoA. Briefly, mitochondria solution (1 mg) was added to the reaction mixture with or without a detergent. Reaction mixture without a detergent contained the following: acetyl coenzyme A (0.3 mM; Sigma-Aldrich, A2056), oxaloacetic acid (5 mM; Sigma-Aldrich, O4126) and 5,5'-dithiobis(2-nitrobenzoic acid) (1 mM; Sigma-Aldrich, D7059). Detergent-added reaction mixture was supplemented with Triton X-100 (0.1%; Sigma-Aldrich, X-100). Absorbance at 412 nm was monitored by spectrophotometer for assessment of 2-nitro-5-benzoic acid production. Outer membrane integrity was spectrophotometrically determined at 30 °C using a Cytochrome C Oxidase Assay Kit (Sigma, CYTOCOX1). Briefly, mitochondria solution (1.5 mg) and mitochondria lysate made with 20 mM n-dodecyl beta D-maltoside (Sigma, D4641) were added to a buffer containing reduced-cytochrome C (0.033 mM; Sigma, C2037). The production of oxidized-cytochrome C was determined by measuring absorbance at 550 nm. Membrane integrity was calculated according to the following formula: membrane integrity (%) = (amount of end product with detergent - amount of end product without detergent) / amount of end product with detergent.

### Isolation and quantification of MRC-Q mtDNA in tissues

Peripheral blood samples were obtained by cardiac puncture. Whole blood was diluted in 1 ml BD Pharm Lyse Lysing buffer (BD Biosciences, 555899) and incubated for 2 min at room temperature to lyse mature erythrocytes. Other tissues were removed after mice were transcardially perfused with PBS. Each tissue was chopped into small pieces with scissors and minced with a homogenizer. Frozen specimens were minced by an ultrasonic homogenizer. DNA was extracted using DNeasy Blood & Tissue Kit (QIAGEN, 69504) according to the manufacturer's instructions. Peripheral blood and BM cells were washed twice in PBS and incubated directly with AL buffer and proteinase K at 56 °C for 10 min. All other tissues were incubated overnight at 56 °C in ATL buffer and proteinase K. The concentration of DNA was determined by a DeNovix spectrophotometer. The isolated DNA samples were stored at -30 °C until further analysis. Quantitative polymerase chain reactions (qPCR) were set using 15 ng of total DNA with TB Green Premix Ex Taq II (Tli RNase H Plus; Takara Bio, RR820W). Human mtDNA (*mt-ND1* and *mt-ND5*) commercial kit primers (human mtDNA monitoring primer set, Takara Bio; 7246) and mouse  $\beta$ -actin fwd (5'-CTAAGGC-CAACCGTGAAAAG-3') and  $\beta$ -actin rev (5'-ACCAGAGGCATACAGG-GACA-3') primers were used. Relative quantification was performed using QuantStudio 1 or QuantStudio 3 Real-Time PCR System (Thermo Fisher Scientific) as follows: an initial denaturation step (95 °C for 1 min) was followed by amplification and quantification steps repeated for 50 cycles (95 °C for 15 s, 60 °C for 1 min). Quadruplicate amplification was carried out for each target gene. Human mtDNA and the mouse nDNA



gene  $\beta$ -actin (Ct) were measured in samples obtained from *Ndufs4*<sup>-/-</sup> mice treated with either MRC-Q or PBS. The human mtDNA signal was normalized to mouse  $\beta$ -actin. For each tissue, the average normalized human mtDNA signal from the PBS  $\rightarrow$  *Ndufs4*<sup>-/-</sup> group (background or non-specific amplification) was subtracted from the normalized human mtDNA signal from each MRC-Q  $\rightarrow$  *Ndufs4*<sup>-/-</sup> sample to obtain a  $\Delta\Delta$ Ct value. Data are expressed as  $2^{-\Delta\Delta$ Ct}.

### Isolation and quantification of NZB mtDNA

Retro-orbital blood was collected and diluted in 250  $\mu$ l of ACK Lysis Buffer (Thermo Fisher, A10492). PECs were obtained with a 7-ml PBS lavage. Mice were perfused with 10 ml of ice-cold PBS via the left ventricle (right ventricle opened) using a peristaltic pump, and heart, lung, liver, spleen, brain and BM were isolated. All samples were placed immediately on dry ice and stored at  $-80^{\circ}\text{C}$ . Frozen tissues were homogenized in 2-ml tubes using 1.4-mm ceramic beads (Fisher Scientific, 15-340-153) and a beadmill homogenizer (Thermo Fisher Scientific). DNA was isolated using the QIAamp DNA mini kit (QIAGEN, 51304) according to manufacturer's instructions. The concentration of DNA in each sample was measured on a BioTek Synergy HI Microplate reader using a Take3 multi-volume plate and Gen5 version 3.11 software. DNA samples were stored at  $-20^{\circ}\text{C}$  until further analysis. qPCR reactions were set up with 100 ng of DNA and PowerUP SYBR Green Master Mix reagent (Thermo, A25742). Primers ARMS22 (5'-TTATCCACGCTCCGTTACGTC-3') and MT20 (5'-TGGCACTCCCCTGTA AAAA-3') were used to amplify NZB mtDNA as previously described<sup>27</sup>, and mouse  $\beta$ -actin fwd (5'-CTAAGGCCAACCGTGA AAAAG-3') and  $\beta$ -actin rev (5'-ACCAGAGGCATACAGG-GACA-3') primers were used to measure nDNA content. qRT-PCR was performed using QuantStudio 3 (Thermo Fisher) with denaturation ( $95^{\circ}\text{C}$  for 1 min) followed by amplification and quantification steps repeated for 40 cycles ( $95^{\circ}\text{C}$  for 15 s,  $62^{\circ}\text{C}$  for 1 min). Reactions were performed in duplicate and averaged. NZB mtDNA (Ct) and the nDNA gene  $\beta$ -actin (Ct) were measured in samples obtained from *Ndufs4*<sup>-/-</sup> mice treated with either NZB mitochondria or C57BL6/J mitochondria. The NZB mtDNA signal was normalized to  $\beta$ -actin. For each tissue, the average normalized NZB mtDNA signal from the B6  $\rightarrow$  *Ndufs4*<sup>-/-</sup> group (background or non-specific amplification) was subtracted from the normalized NZB mtDNA signal from each NZB  $\rightarrow$  *Ndufs4*<sup>-/-</sup> sample to obtain a  $\Delta\Delta$ Ct value. Data are expressed as  $2^{-\Delta\Delta$ Ct}.

### Isolation of RNA and real-time RT-qPCR

Tissues were homogenized as described above, and RNA was isolated using the Direct-zol RNA MiniPrep Plus kit (Zymo, R2072) according to manufacturer's instructions. For PECS, RNA was isolated using the RNeasy Micro Kit (QIAGEN, 74004) according to the manufacturer's instructions. The concentration of RNA in each sample was measured on a BioTek Synergy HI Microplate reader using a Take3 multi-volume plate and Gen5 3.11 software. RNA samples were converted to cDNA using the SuperScript IV VILO Master Mix (Thermo Fisher, 11766050) according to manufacturer's instructions. qRT-PCR was performed using the following primers: *Il6* fwd (5'-GACAACCTTGGCATTGTGG-3'), *Il6* rev (5'-ATGCAGGGATGATGTTCTG-3'); *Il18* fwd (5'-GACTCTTCGCTCAACTTCAAGG-3'), *Il18* rev (5'-CAGGCTGTCTTTGTCAACGA-3'); *Tnf* fwd (5'-TATGGCCAGACCCTCACA-3'), *Tnf* rev (5'-GGAGTAGACAAAGGTACAACCCATC-3'); *Ifng* fwd (ATTGCGGGTGTATCTGGG), *Ifng* rev (GGGTCAGTGCAGCTCTGAAT); *Il-4* fwd (5'-AGATGGATGTGC-CAAACGTCCTCA-3'), *Il-4* rev (5'-AATATGCCAAGCACCTTGGAAGCC-3'); and  $\beta$ -actin fwd (5'-CTAAGGCCAACCGTGA AAAAG-3'),  $\beta$ -actin rev (5'-ACCAGAGGCATACAGGGACA-3') using a QuantStudio 3 (Thermo Fisher) with an initial denaturation step ( $95^{\circ}\text{C}$  for 1 min) followed by amplification repeated for 40 cycles ( $95^{\circ}\text{C}$  for 15 s,  $60^{\circ}\text{C}$  for 1 min). Reactions were performed in duplicate and averaged. The relative expression was calculated by the  $\Delta\Delta$ Ct method.  $\beta$ -actin was used for normalization, and data are expressed as a fold change relative to the control group using  $2^{-\Delta\Delta$ Ct}.

### Statistics

Each experiment was performed in 2–5 independent cohorts and data were pooled for statistical analyses. All statistical tests were two sided. Two-group comparisons were made using two-way Student's *t*-tests if normally distributed, with Welch's correction applied when the variance between groups differed. The Mann-Whitney test was used for nonparametric comparisons of two groups. Energy expenditure over time was compared using a two-way ANOVA with repeated measures. Immune cell frequencies and numbers were compared using a two-way ANOVA with Sidak post hoc test. Survival was compared using the Mantel-Cox log-rank test. Power calculations were performed to estimate the minimum sample sizes needed to achieve at least 80% power with statistical significance set at 0.05 for the primary outcomes (survival or degree of mitochondria transfer). Data are expressed as the mean  $\pm$  s.e.m. The threshold for significance was  $P < 0.05$ . Data analyses were performed using Prism v9 or v10 (GraphPad) and Excel v16.74 (Microsoft).

### Reporting summary

Further information on research design is available in the Nature Portfolio Reporting Summary linked to this article.

### Data availability

All data supporting the findings of this study are available within the paper and its Supplementary Information or are available by request to the corresponding authors. MRC-Q is a proprietary, unique biological material and its use is restricted by a material transfer agreement. MRC-Q is available upon request from LUCA Science. Source data are provided with this paper.

### References

- Al Amir Dache, Z. & Thierry, A. R. Mitochondria-derived cell-to-cell communication. *Cell Rep.* **42**, 112728 (2023).
- Zhu, M. et al. Mitochondria released by apoptotic cell death initiate innate immune responses. *Immunohorizons* **2**, 384–397 (2018).
- Borcherding, N. & Brestoff, J. R. The power and potential of mitochondria transfer. *Nature* **623**, 283–291 (2023).
- Borcherding, N. et al. Dietary lipids inhibit mitochondria transfer to macrophages to divert adipocyte-derived mitochondria into blood. *Cell Metab.* **34**, 1499–1513.e8 (2022).
- Spees, J. L., Olson, S. D., Whitney, M. J. & Prockop, D. J. Mitochondrial transfer between cells can rescue aerobic respiration. *Proc. Natl Acad. Sci. USA* **103**, 1283–1288 (2006).
- Kim, M. J., Hwang, J. W., Yun, C.-K., Lee, Y. & Choi, Y.-S. Delivery of exogenous mitochondria via centrifugation enhances cellular metabolic function. *Sci. Rep.* **8**, 3330 (2018).
- Caicedo, A. et al. MitoCeption as a new tool to assess the effects of mesenchymal stem/stromal cell mitochondria on cancer cell metabolism and function. *Sci. Rep.* **5**, 9073 (2015).
- Jacoby, E. et al. Mitochondrial augmentation of hematopoietic stem cells in children with single large-scale mitochondrial DNA deletion syndromes. *Sci. Transl. Med.* **14**, eabo3724 (2022).
- Jacoby, E. et al. Mitochondrial augmentation of CD34<sup>+</sup> cells from healthy donors and patients with mitochondrial DNA disorders confers functional benefit. *NPJ Regen. Med.* **6**, 58 (2021).
- Masuzawa, A. et al. Transplantation of autologously derived mitochondria protects the heart from ischemia-reperfusion injury. *Am. J. Physiol. Heart Circ. Physiol.* **304**, H966–H982 (2013).
- McCully, J. D. et al. Injection of isolated mitochondria during early reperfusion for cardioprotection. *Am. J. Physiol. Heart Circ. Physiol.* **296**, H94–H105 (2009).
- Emani, S. M., Piekarski, B. L., Harrild, D., Nido, P. J. D. & McCully, J. D. Autologous mitochondrial transplantation for dysfunction after ischemia-reperfusion injury. *J. Thorac. Cardiovasc. Surg.* **154**, 286–289 (2017).

13. Hayakawa, K. et al. Protective effects of endothelial progenitor cell-derived extracellular mitochondria in brain endothelium. *Stem Cells* **36**, 1404–1410 (2018).
14. Hayakawa, K. et al. Transfer of mitochondria from astrocytes to neurons after stroke. *Nature* **535**, 551–555 (2016).
15. Norat, P. et al. Intraarterial transplantation of mitochondria after ischemic stroke reduces cerebral infarction. *Stroke Vasc. Interv. Neurol.* **3**, e000644 (2023).
16. Lin, R. Z. et al. Mitochondrial transfer mediates endothelial cell engraftment through mitophagy. *Nature* **629**, 660–668 (2024).
17. Diodato, D. et al. 25th ENMC international workshop Leigh syndrome spectrum: genetic causes, natural history and preparing for clinical trials 25–27 March 2022, Hoofddorp, Amsterdam, The Netherlands. *Neuromuscul. Disord.* <https://doi.org/10.1016/j.nmd.2023.06.002> (2023).
18. Sofou, K. et al. A multicenter study on Leigh syndrome: disease course and predictors of survival. *Orphanet J. Rare Dis.* **9**, 52 (2014).
19. McCormick, E. M. et al. Expert panel curation of 113 primary mitochondrial disease genes for the Leigh syndrome spectrum. *Ann. Neurol.* **94**, 696–712 (2023).
20. Kruse, S. E. et al. Mice with mitochondrial complex I deficiency develop a fatal encephalomyopathy. *Cell Metab.* **7**, 312–320 (2008).
21. Pham, A. H., McCaffery, J. M. & Chan, D. C. Mouse lines with photo-activatable mitochondria to study mitochondrial dynamics. *Genesis* **50**, 833–843 (2012).
22. Brestoff, J. R. et al. Intercellular mitochondria transfer to macrophages regulates white adipose tissue homeostasis and is impaired in obesity. *Cell Metab.* **33**, 270–282.e8 (2021).
23. Boudreau, L. H. et al. Platelets release mitochondria serving as substrate for bactericidal group IIA-secreted phospholipase A2 to promote inflammation. *Blood* **124**, 2173–2183 (2014).
24. Dache, Z. A. A. et al. Blood contains circulating cell-free respiratory competent mitochondria. *FASEB J.* **34**, 3616–3630 (2020).
25. Crewe, C. et al. Extracellular vesicle-based interorgan transport of mitochondria from energetically stressed adipocytes. *Cell Metab.* **33**, 1853–1868.e11 (2021).
26. van der Vlist, M. et al. Macrophages transfer mitochondria to sensory neurons to resolve inflammatory pain. *Neuron* **110**, 613–626.e9 (2022).
27. Machado, T. S. et al. Real-time PCR quantification of heteroplasmy in a mouse model with mitochondrial DNA of C57BL/6 and NZB/BINJ strains. *PLoS ONE* **10**, e0133650 (2015).
28. Court, A. C. et al. Mitochondrial transfer from MSCs to T cells induces T<sub>reg</sub> differentiation and restricts inflammatory response. *EMBO Rep.* **21**, e48052 (2020).
29. Luz-Crawford, P. et al. Mesenchymal stem cell repression of T<sub>H</sub>17 cells is triggered by mitochondrial transfer. *Stem Cell Res. Ther.* **10**, 232 (2019).
30. Wu, B. et al. Mitochondrial aspartate regulates TNF biogenesis and autoimmune tissue inflammation. *Nat. Immunol.* **22**, 1551–1562 (2021).
31. Peruzzotti-Jametti, L. et al. Neural stem cells traffic functional mitochondria via extracellular vesicles. *PLoS Biol.* **19**, e3001166 (2021).
32. Stokes, J. C. et al. Leukocytes mediate disease pathogenesis in the *Ndufs4*(KO) mouse model of Leigh syndrome. *JCI Insight* <https://doi.org/10.1172/jci.insight.156522> (2022).
33. Jin, Z., Wei, W., Yang, M., Du, Y. & Wan, Y. Mitochondrial complex I activity suppresses inflammation and enhances bone resorption by shifting macrophage-osteoclast polarization. *Cell Metab.* **20**, 483–498 (2014).
34. Yu, A. K. et al. Mitochondrial complex I deficiency leads to inflammation and retinal ganglion cell death in the *Ndufs4* mouse. *Hum. Mol. Genet.* **24**, 2848–2860 (2015).
35. Yoon, Y. G., Haug, C. L. & Koob, M. D. Interspecies mitochondrial fusion between mouse and human mitochondria is rapid and efficient. *Mitochondrion* **7**, 223–229 (2007).
36. Jain, I. H. et al. Leigh Syndrome Mouse Model Can Be Rescued by Interventions that Normalize Brain Hyperoxia, but Not HIF Activation. *Cell Metab.* **30**, 824–832.e3 (2019).
37. McElroy, G. S. et al. NAD<sup>+</sup> regeneration rescues lifespan, but not ataxia, in a mouse model of brain mitochondrial complex I dysfunction. *Cell Metab.* **32**, 301–308.e6 (2020).
38. Lee, C. F., Caudal, A., Abell, L., Nagana Gowda, G. A. & Tian, R. Targeting NAD<sup>+</sup> metabolism as interventions for mitochondrial disease. *Sci. Rep.* **9**, 3073 (2019).
39. Ball, M., Thorburn, D. R. & Rahman, S. in *GeneReviews* (eds Adam, M. P. et al.) 1993–2024 (Univ. Washington, 2003).
40. Daemen, S., Chan, M. M. & Schilling, J. D. Comprehensive analysis of liver macrophage composition by flow cytometry and immunofluorescence in murine NASH. *STAR Protoc.* **2**, 100511 (2021).

## Acknowledgements

Funding for this study was provided by the National Institute of Neurological Disorders and Stroke award 1R01NS134932 (to J.R.B.), Burroughs Wellcome Fund Career Award for Medical Scientists no. 1019648 (to J.R.B.) and a Grant-in-Aid for Scientific Research (C) 21K08415 (to T.Y.). Additional support was provided by the Japanese Society of Hematology (to R.N.), JST SPRING JPMJSP no. 2138 (to R.N.), the Japan Society for the Promotion of Science KAKENHI 20K17379 (to R.N.) and 22K16322 (to R.N.), American Heart Association (AHA) Predoctoral Fellowship 24PRE1189775 (to R.G.), AHA Postdoctoral Fellowship 24POST1244220 (to W.J.), W.M. Keck Foundation Fellowship in Molecular Medicine (to S.J.K.), a Washington University BioSURF grant (to E.F.C.) and National Institutes of Health (NIH) 5U54-NS078059-12 (to R.P.S.). We thank LUCA Science staff T. Shibata for developing the MRC-Q isolation method, J. Hayashi for providing MRC-Q materials and Y. El-Darawish for developing methods. Experimental design schematics in Figs. 1a, 2a, 3a,f,h and 4d were created with [BioRender.com](https://BioRender.com).

## Author contributions

R.N. and S.V. performed experiments, analysed data, interpreted results and wrote the manuscript. R.L.F., H.S., R.G., W.J., S.J.K., E.F.C. and N.B. performed experiments, analysed data and interpreted results. R.P.S. provided scientific guidance and interpreted results. R.C.T., M.S. and H.O. gave scientific guidance, provided essential reagents, performed experiments and interpreted results. T.Y. and J.R.B. conceived of the project, secured funding, performed experiments, interpreted results and wrote the manuscript. All authors contributed to writing, editing and/or revising this manuscript and approved the final version.

## Competing interests

R.C.T., H.O. and M.S. are employees of LUCA Science and are inventors on patents and/or pending patents related to MRC-Q (WO2024010862, WO2024010866). J.R.B. has pending patent applications related to the treatment of obesity (63/625,555) and allergic diseases (US20210128689A1), is a consultant for Columbus Instruments, has been a consultant for DeciBio in the past 12 months, is a member of the Scientific Advisory Board for LUCA Science, receives research support from LUCA Science for a project unrelated to this paper and receives royalties from Springer Nature Group. J.R.B., N.B. and R.L.F. are inventors of technology (Clambake) licensed to Columbus Instruments, which is not used in this paper. N.B. was employed by Omniscope within the past 12 months and holds equity in this company. R.P.S. receives research funding from Astellas (0367-CL-1201) that is unrelated to this paper. R.N. and T.Y. receive research support from LUCA Science. All other authors declare no competing interests.

## Additional information

**Extended data** is available for this paper at <https://doi.org/10.1038/s42255-024-01125-5>.

**Supplementary information** The online version contains supplementary material available at <https://doi.org/10.1038/s42255-024-01125-5>.

**Correspondence and requests for materials** should be addressed to Takafumi Yokota or Jonathan R. Brestoff.

**Peer review information** *Nature Metabolism* thanks Alessandro Bitto, Anne-Marie Rodriguez and the other, anonymous, reviewer(s) for their contribution to the peer review of this work. Primary Handling Editor: Christoph Schmitt, in collaboration with the *Nature Metabolism* team.





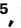


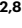


**Reprints and permissions information** is available at [www.nature.com/reprints](http://www.nature.com/reprints).

**Publisher's note** Springer Nature remains neutral with regard to jurisdictional claims in published maps and institutional affiliations.

Springer Nature or its licensor (e.g. a society or other partner) holds exclusive rights to this article under a publishing agreement with the author(s) or other rightsholder(s); author self-archiving of the accepted manuscript version of this article is solely governed by the terms of such publishing agreement and applicable law.

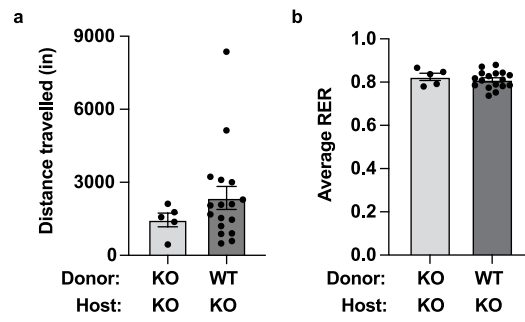
© The Author(s), under exclusive licence to Springer Nature Limited 2024

---

**Ritsuko Nakai** <sup>1,2,3,7</sup>, **Stella Varnum** <sup>4,7</sup>, **Rachael L. Field** <sup>4</sup>, **Henry Shi**<sup>1,2</sup>, **Rocky Giwa**<sup>4</sup>, **Wentong Jia**<sup>4</sup>, **Samantha J. Krysa**<sup>4</sup>, **Eva F. Cohen**<sup>4</sup>, **Nicholas Borchering**<sup>4</sup>, **Russell P. Saneto** <sup>5</sup>, **Rick C. Tsai** <sup>6</sup>, **Masashi Suganuma** <sup>6</sup>, **Hisashi Ohta**<sup>6</sup>, **Takafumi Yokota** <sup>1,2,8</sup>  & **Jonathan R. Brestoff** <sup>4,8</sup> 

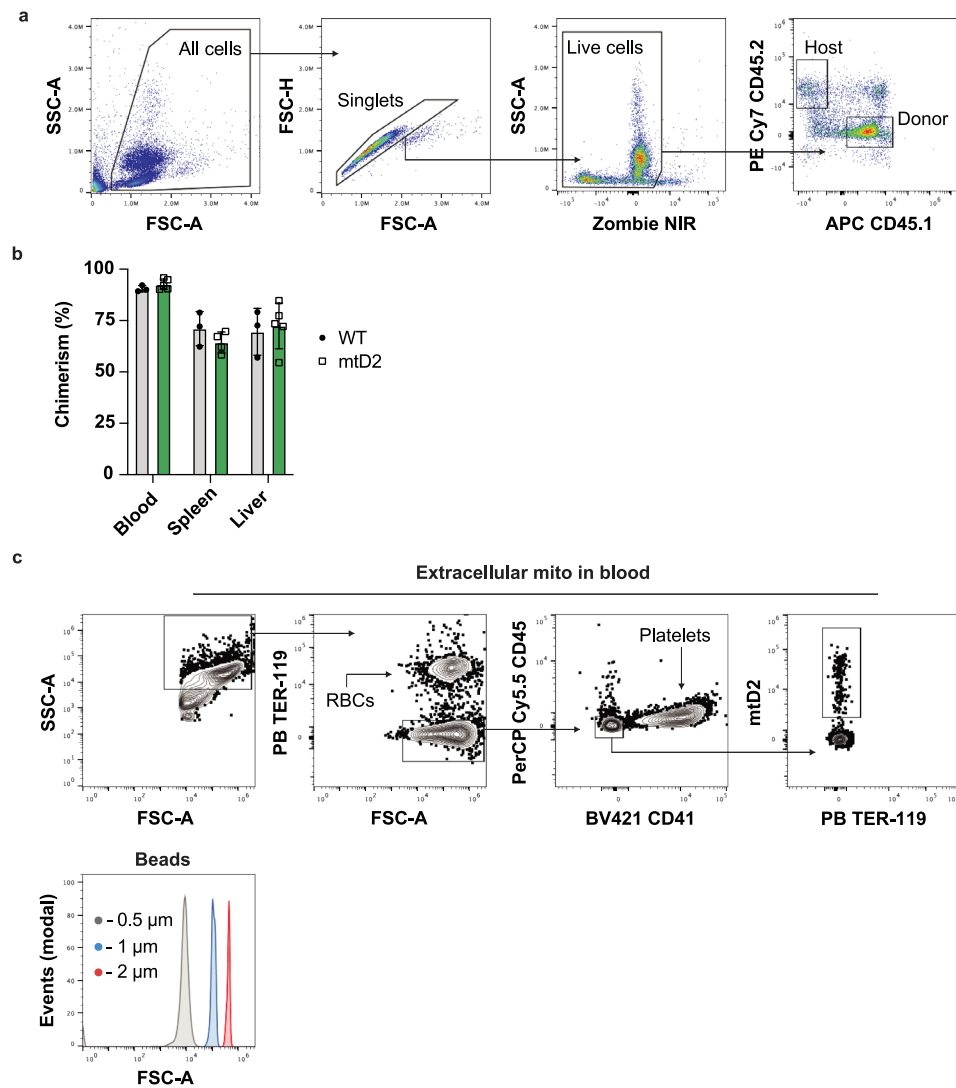
---

<sup>1</sup>Department of Hematology and Oncology, Graduate School of Medicine, Osaka University, Suita, Japan. <sup>2</sup>Department of Hematology, Osaka International Cancer Institute, Osaka, Japan. <sup>3</sup>Department of Hematology, Sakai City Medical Center, Sakai, Japan. <sup>4</sup>Department of Pathology and Immunology, Washington University School of Medicine, St. Louis, MO, USA. <sup>5</sup>Neuroscience Institute, Center for Integrated Brain Research, Seattle Children's Hospital, University of Washington, Seattle, WA, USA. <sup>6</sup>LUCA Science, Tokyo, Japan. <sup>7</sup>These authors contributed equally: Ritsuko Nakai, Stella Varnum. <sup>8</sup>These authors jointly supervised this work: Takafumi Yokota, Jonathan R. Brestoff. ✉e-mail: [yokotat@oici.jp](mailto:yokotat@oici.jp); [brestoff@wustl.edu](mailto:brestoff@wustl.edu)



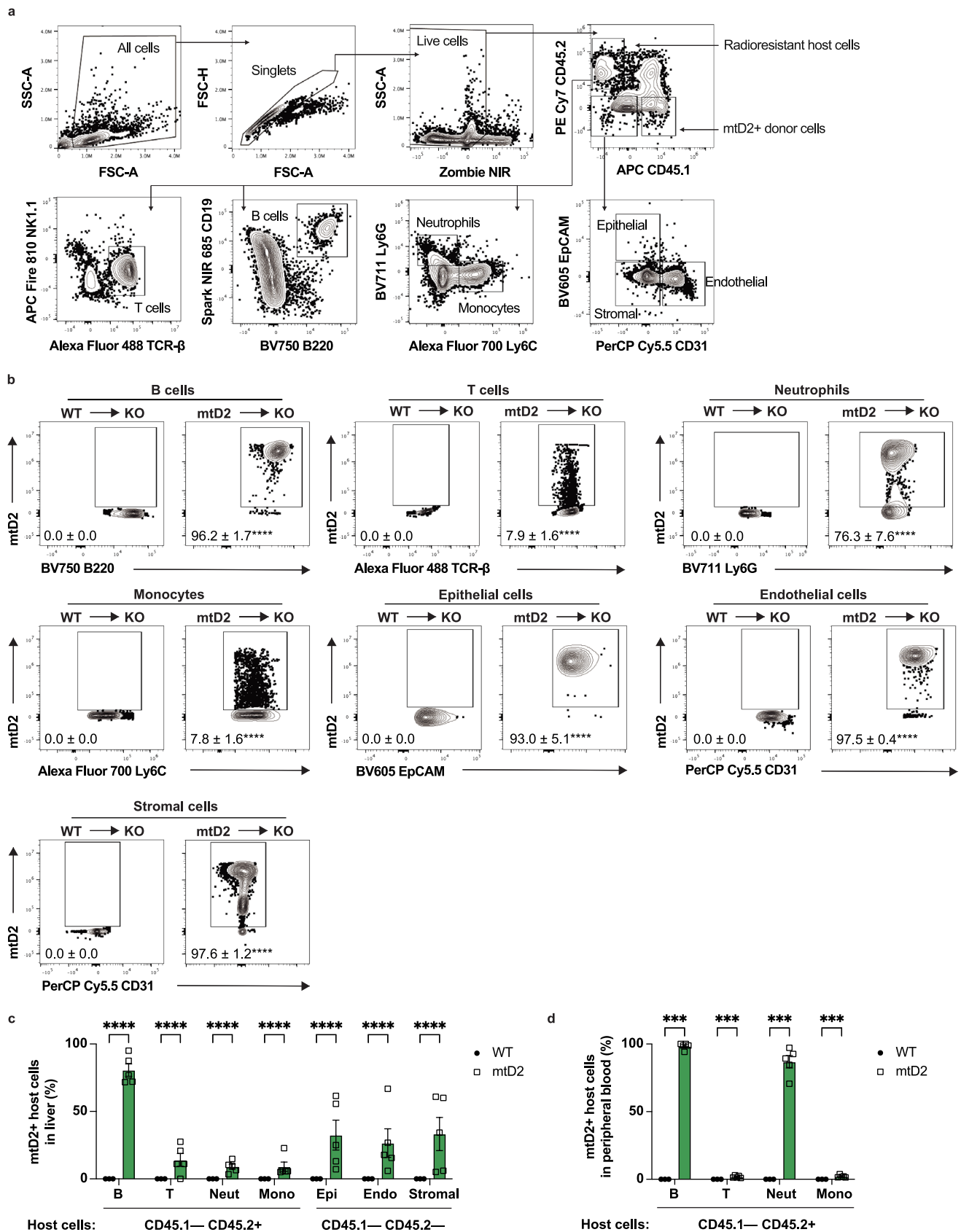
**Extended Data Fig. 1 | Additional metabolic cage parameters from NDUFS4-deficient mice treated with wildtype or NDUFS4-deficient bone marrow transplantation. (a)** Distance travelled and **(b)** average respiratory

exchange ratio (RER) over 3 hr after a 1 hr air equilibration period. Data are expressed as mean  $\pm$  SEM. All data points are unique biological replicates.  $n = 5$  KO,  $n = 17$  WT. Data accompanies Fig. 1.



gating in the blood to exclude red blood cells (RBCs) and platelets from particles less than 2  $\mu\text{m}$  in diameter for identification of extracellular mtD2<sup>+</sup> mitochondria. Data are expressed as mean  $\pm$  SEM. All data points are unique biological replicates. For b, n = 3 WT, n = 5 mtD2 (except n = 4 for spleen). Data accompanies Fig. 2.

gating in the blood to exclude red blood cells (RBCs) and platelets from particles less than 2  $\mu\text{m}$  in diameter for identification of extracellular mtD2<sup>+</sup> mitochondria. Data are expressed as mean  $\pm$  SEM. All data points are unique biological replicates. For b, n = 3 WT, n = 5 mtD2 (except n = 4 for spleen). Data accompanies Fig. 2.

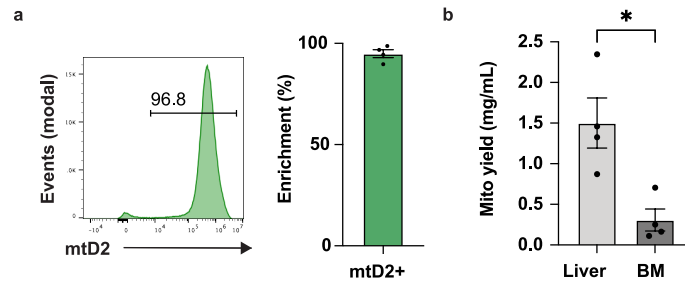


Extended Data Fig. 3 | See next page for caption.

**Extended Data Fig. 3 | Bone marrow transplantation leads to transfer of mtD2+ mitochondria to host cells in the blood, spleen, and liver. (a)**

Representative gating for identification of CD45.1<sup>-</sup> CD45.2<sup>+</sup> radioresistant host B cells, T cells, neutrophils, and monocytes as well as CD45.1<sup>-</sup> CD45.2<sup>-</sup> host epithelial, endothelial, and stromal cells in the spleen. **(b)** Representative gating to identify the proportions of host B cells, T cells, neutrophils, monocytes, epithelial, endothelial, and stromal cells that received mtD2<sup>+</sup> mitochondria in the

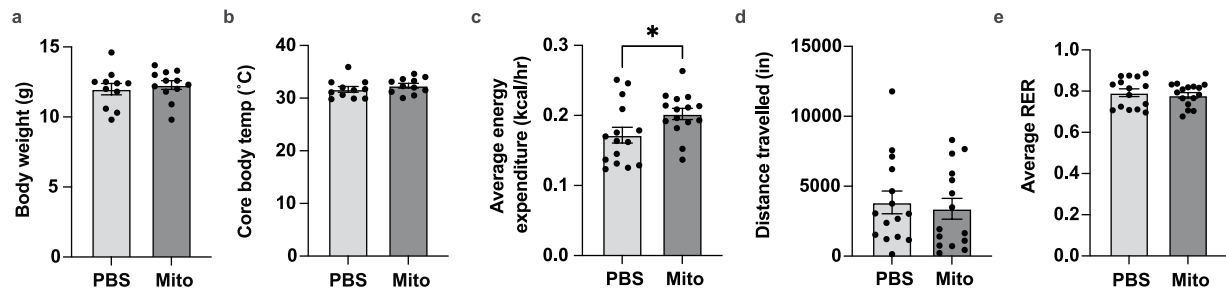
spleen. **(c)** Proportions of B cells (B), T cells (T), neutrophils (neut), monocytes (mono), epithelial cells (epi), endothelial cells (endo), and stromal cells that received mtD2<sup>+</sup> mitochondria in the liver and **(d)** peripheral blood. For c-d, closed circles are WT and open squares are mtD2. Data are expressed as mean  $\pm$  SEM. All data points are unique biological replicates. For b-d, n=3 WT, n=5 mtD2 (except n=4 for spleen). For b-d, 2-way ANOVA with Sidak post-hoc test. \*\*\*P<0.001, \*\*\*\*P<0.0001. Data accompanies Fig. 2.



**Extended Data Fig. 4 | Mitochondria isolates from the liver are enriched in mtD2<sup>+</sup> events and produce more yield than bone marrow mitochondria isolates. (a)** Flow cytometric identification of the proportion of mtD2<sup>+</sup> mitochondria. Pre-gated on CD41<sup>-</sup> CD45<sup>-</sup> TER-119<sup>-</sup> events less than 2 μm in

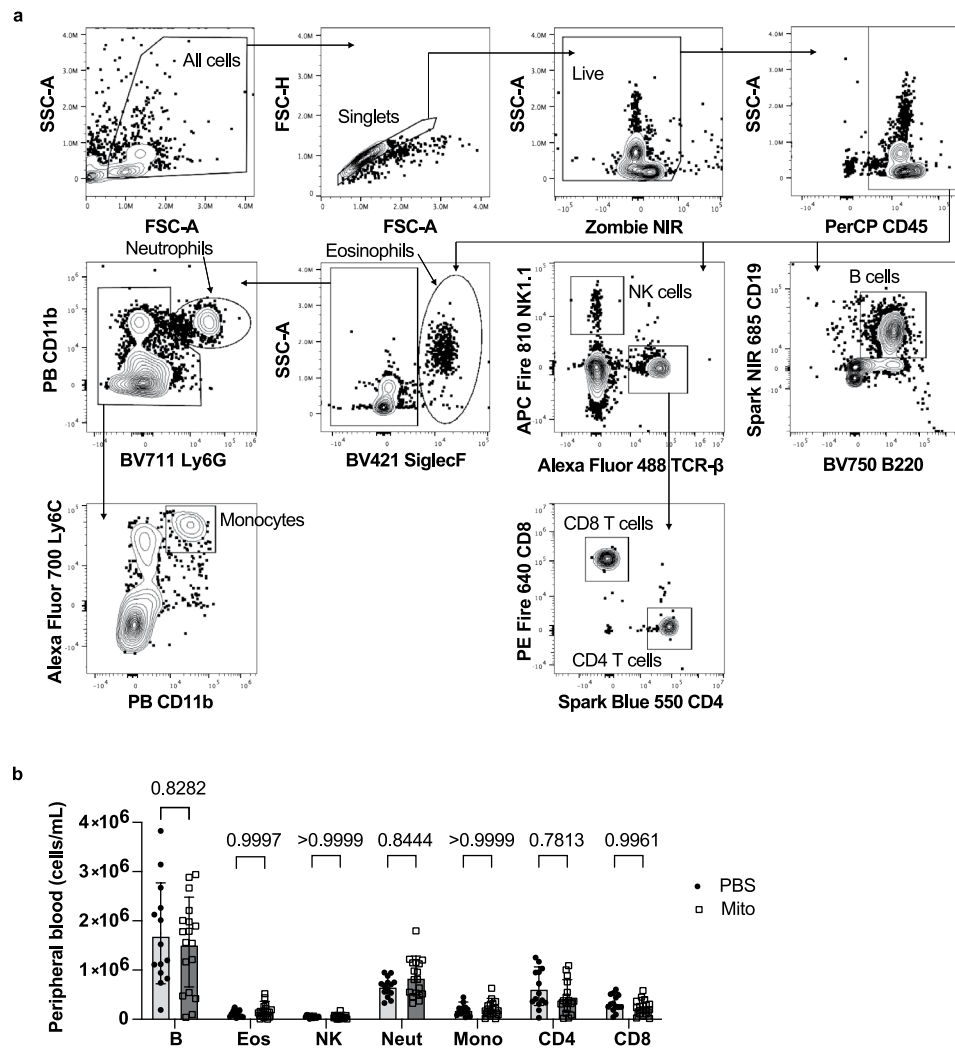
diameter. **(b)** Mitochondrial yield from mouse liver or bone marrow (BM). Data are expressed as mean +/- SEM. All data points are unique biological replicates. For a-b, n=4 biological replicates/group. For b, Student's *t*-test (two-sided). \*P<0.05 Data accompanies Fig. 3.





**Extended Data Fig. 5 | Additional metabolic cage parameters from NDUFS4-deficient mice treated with mitochondria or PBS.** (a) Body weight, and (b) rectal core body temperature of 7-week-old KO mice treated with PBS or 100  $\mu$ g mitochondria 1-2 times per week. (c) Average energy expenditure (d) distance travelled, and (e) average respiratory exchange ratio (RER) over 3 hr after a 1 hr

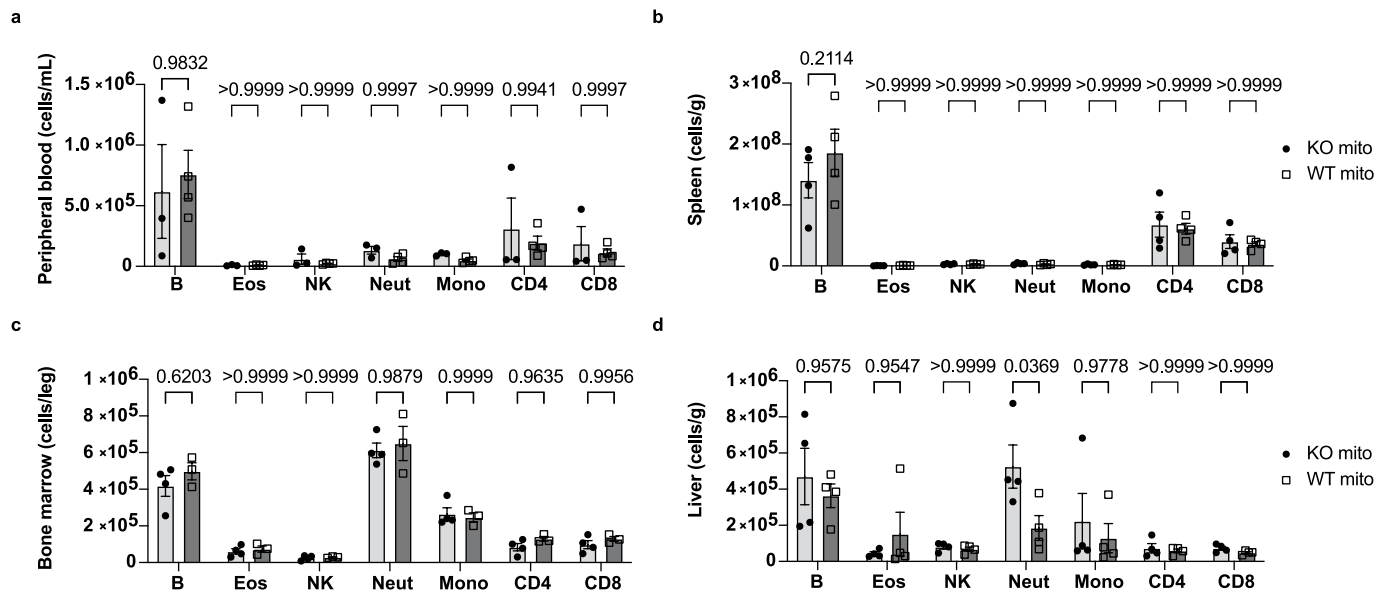
air equilibration period. Data are expressed as mean  $\pm$  SEM. All data points are unique biological replicates. For a,  $n = 11$  PBS,  $n = 12$  WT. For b,  $n = 11$ /group. For c-e,  $n = 15$ /group. Variation in  $n$  is due to mouse mortality. For c, Student's  $t$ -test (two-sided). \* $P < 0.05$ . Data accompanies Fig. 3.



**Extended Data Fig. 6 | Administration of wildtype mitochondria to *NDUFS4*-deficient mice does not alter immune cell composition in the blood. (a)**

Representative gating to identify immune cells in the peripheral blood of *Ndufs4*<sup>-/-</sup> (KO) mice. **(b)** Overall number of B cells (B), eosinophils (eos), natural killer cells (NK), neutrophils (neut), monocytes (mono), CD4 T cells, and CD8 T

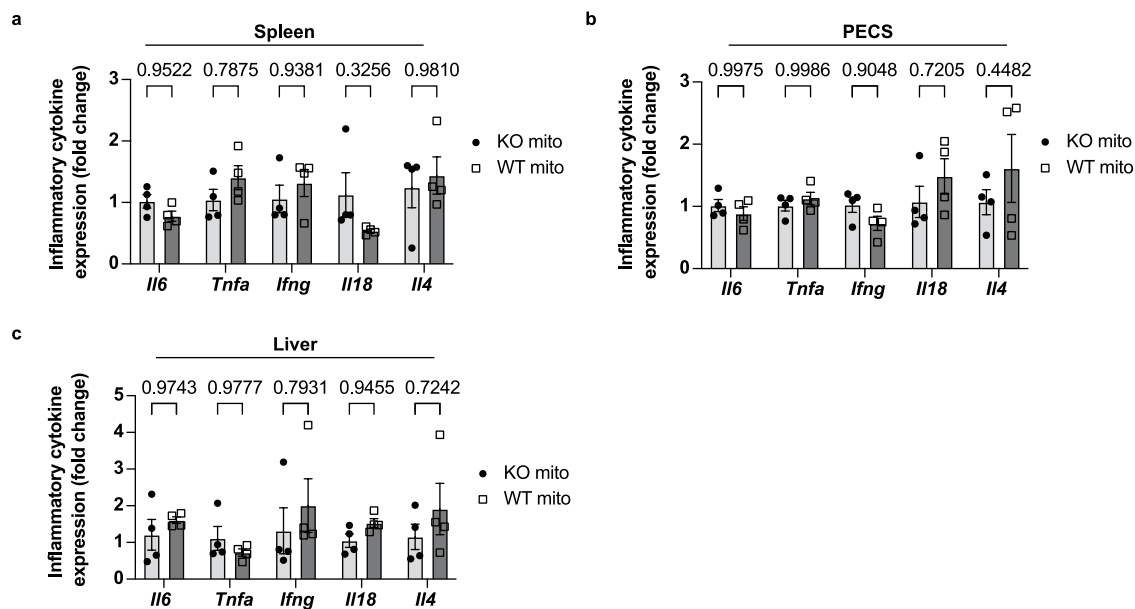
cells per mL of peripheral blood from KO mice treated weekly with PBS (closed circle) or 100 μg mitochondria (open square) for 5 weeks. Data are expressed as mean ± SEM. All data points are unique biological replicates. For b, n=14 PBS, n=18 Mito. For b, 2-way ANOVA with Sidak post-hoc test. Data accompanies Fig. 3.



**Extended Data Fig. 7 | Administration of mitochondria to NDUFS4-deficient mice does not alter immune cell composition in the blood or tissues.**

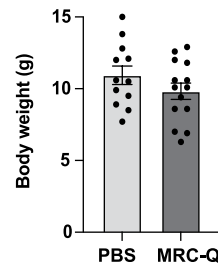
Overall number of immune cells in peripheral blood, (b) spleen, (c) bone marrow, and (d) liver of *Ndufs4*<sup>-/-</sup> mice treated weekly with 100 μg KO or WT mitochondria for 7 weeks. For a-d, closed circles are KO mito and open squares are WT mito.

Data are expressed as mean ± SEM. All data points are unique biological replicates. For a, n=3 KO Mito, n=4 WT Mito. For b and d, n=4/group. For c, n=4 KO Mito, n=3 WT Mito. For a-d, 2-way ANOVA with Sidak post-hoc test. Data accompanies Fig. 3.



**Extended Data Fig. 8 | Administration of mitochondria to NDUF54-deficient mice does not alter expression of inflammatory cytokines.** (a) Inflammatory cytokine expression in the spleen (b) peritoneal exudate cells (PECS), and (c) liver of *Ndufs4*<sup>-/-</sup> mice treated weekly with 100 $\mu$ g KO or WT mitochondria for 7

weeks. For a-c, closed circles are KO mito and open squares are WT mito. Data are expressed as mean  $\pm$  SEM. All data points are unique biological replicates. For a-c, n=4 biological replicates/group. For a-c, 2-way ANOVA with Sidak post-hoc test. Data accompanies Fig. 3.



**Extended Data Fig. 9 | Administration of MRC-Q does not alter body weight in NDUF54-deficient mice.** Body weight of *Ndufs4*<sup>-/-</sup> mice treated with PBS or 50  $\mu$ g MRC-Q once per week from 3- to 7-weeks old. Data are expressed as mean  $\pm$  SEM. All data points are unique biological replicates. n = 12 PBS, n = 14 MRC-Q. Data accompanies Fig. 4.

Extended Data Table 1 | Comparison of the three treatment paradigms and their outcomes

		Figure 1	Figure 3	Figure 4
Experimental parameters:	Treatment paradigm	BMT	Mitochondria transplant	
	Irradiation of treated mice	Yes	No	No
	Bone marrow cells	Yes	No	No
	Mitochondria transplant	No	Yes	Yes
	Donor species	Mouse	Mouse	Human
	Mitochondria dose	n/a	PBS: 0 Mito: 100 µg	PBS: 0 MRC-Q: 50 µg
	Performance sites	WUSM, OU	WUSM	OU
Survival outcomes:	Median survival (days)	KO to KO: 40 WT to KO: 74	PBS: 68 Mito: 84	PBS: 67.5 MRC-Q: 80.5
	Sample size per group (n)	KO to KO: 11 WT to KO: 29	PBS: 27 Mito: 23	PBS: 14 MRC-Q: 14
	P-value, Mantel-Cox logrank test of survival curves	<0.0001	0.0052	0.0079

Abbreviations: BMT, bone marrow transplant; n/a, not applicable; PBS, phosphate buffered saline; Mito, mitochondria; WUSM, Washington University School of Medicine; OU, Osaka University; WT, wildtype; KO, knockout (of *Ndufs4*)

## Reporting Summary

Nature Portfolio wishes to improve the reproducibility of the work that we publish. This form provides structure for consistency and transparency in reporting. For further information on Nature Portfolio policies, see our [Editorial Policies](#) and the [Editorial Policy Checklist](#).

### Statistics

For all statistical analyses, confirm that the following items are present in the figure legend, table legend, main text, or Methods section.

- | n/a                                 | Confirmed  |
|-------------------------------------|--|
| <input type="checkbox"/>            | <input checked="" type="checkbox"/> The exact sample size ( $n$ ) for each experimental group/condition, given as a discrete number and unit of measurement  |
| <input type="checkbox"/>            | <input checked="" type="checkbox"/> A statement on whether measurements were taken from distinct samples or whether the same sample was measured repeatedly  |
| <input type="checkbox"/>            | <input checked="" type="checkbox"/> The statistical test(s) used AND whether they are one- or two-sided<br><i>Only common tests should be described solely by name; describe more complex techniques in the Methods section.</i>   |
| <input type="checkbox"/>            | <input checked="" type="checkbox"/> A description of all covariates tested   |
| <input type="checkbox"/>            | <input checked="" type="checkbox"/> A description of any assumptions or corrections, such as tests of normality and adjustment for multiple comparisons  |
| <input type="checkbox"/>            | <input checked="" type="checkbox"/> A full description of the statistical parameters including central tendency (e.g. means) or other basic estimates (e.g. regression coefficient) AND variation (e.g. standard deviation) or associated estimates of uncertainty (e.g. confidence intervals) |
| <input type="checkbox"/>            | <input checked="" type="checkbox"/> For null hypothesis testing, the test statistic (e.g. $F$ , $t$ , $r$ ) with confidence intervals, effect sizes, degrees of freedom and $P$ value noted<br><i>Give <math>P</math> values as exact values whenever suitable.</i>                            |
| <input checked="" type="checkbox"/> | <input type="checkbox"/> For Bayesian analysis, information on the choice of priors and Markov chain Monte Carlo settings  |
| <input checked="" type="checkbox"/> | <input type="checkbox"/> For hierarchical and complex designs, identification of the appropriate level for tests and full reporting of outcomes  |
| <input checked="" type="checkbox"/> | <input type="checkbox"/> Estimates of effect sizes (e.g. Cohen's $d$ , Pearson's $r$ ), indicating how they were calculated  |

*Our web collection on [statistics for biologists](#) contains articles on many of the points above.*

### Software and code

Policy information about [availability of computer code](#)

- |                 |  |
|-----------------|--|
| Data collection | Flow cytometry data were collected using SpectroFlo 2.0 (Cytex Biosciences). Metabolic cage data were collected using OxyMax v5.66 software (Columbus Instruments). Grip strength data were generated using BIO-CIS v1.5.1.0(En) software (Bioseb). Plate reader absorbance data were generated using Gen5 v3.11 (BioTek). |
| Data analysis   | Data were analyzed using Prism v9 or v10 (GraphPad) and Excel v16.74 (Microsoft). Flow cytometry data were also analyzed using FlowJo v10.8 or v10.9   |

For manuscripts utilizing custom algorithms or software that are central to the research but not yet described in published literature, software must be made available to editors and reviewers. We strongly encourage code deposition in a community repository (e.g. GitHub). See the Nature Portfolio [guidelines for submitting code & software](#) for further information.

### Data

Policy information about [availability of data](#)

All manuscripts must include a [data availability statement](#). This statement should provide the following information, where applicable:

- Accession codes, unique identifiers, or web links for publicly available datasets
- A description of any restrictions on data availability
- For clinical datasets or third party data, please ensure that the statement adheres to our [policy](#)

All data supporting the findings of this study are available within the paper and its Supplementary Information or are available by request to the corresponding

authors. MRC-Q is a proprietary, unique biological material and its use is restricted by a material transfer agreement. MRC-Q is available upon request from LUCA Science, Inc. authors. This study does not include use of new code. MRC-Q is proprietary unique biological material and its use is restricted by a material transfer agreement. MRC-Q is available upon request from LUCA Science, Inc.

## Research involving human participants, their data, or biological material

Policy information about studies with [human participants or human data](#). See also policy information about [sex, gender \(identity/presentation\), and sexual orientation](#) and [race, ethnicity and racism](#).

Reporting on sex and gender	n/a
Reporting on race, ethnicity, or other socially relevant groupings	n/a
Population characteristics	n/a
Recruitment	n/a
Ethics oversight	n/a

Note that full information on the approval of the study protocol must also be provided in the manuscript.

## Field-specific reporting

Please select the one below that is the best fit for your research. If you are not sure, read the appropriate sections before making your selection.

Life sciences  Behavioural & social sciences  Ecological, evolutionary & environmental sciences

For a reference copy of the document with all sections, see [nature.com/documents/nr-reporting-summary-flat.pdf](https://www.nature.com/documents/nr-reporting-summary-flat.pdf)

## Life sciences study design

All studies must disclose on these points even when the disclosure is negative.

Sample size	Minimum sample sizes were determined based on initial pilot studies to generate preliminary estimates of means and standard deviations of the primary outcome, which in Figs 1, 3, and 4 was survival. In Fig 2, the primary outcome was % of recipient cells that were mtD2+, for which we had preliminary data from a prior publication (Brestoff et al., Cell Metabolism, 2021) to perform power calculations. Using well-established power calculations (Brestoff & Van den Broeck, "Chapter 7: Study Size Planning." Epidemiology: Principles and Practical Guidelines, Eds. Brestoff JR & Van den Broeck. Springer Science+Business Media: Dordrecht, 2013.), we estimated the number of animals required assuming 80% power and significance of 0.05.
Data exclusions	There were no data exclusions. However, the number of data points may vary from panel to panel within a figure because the Ndufs4-deficient mice die from Leigh Syndrome and therefore drop out. There was preferential death in the control groups, therefore sample sizes for the controls groups are often lower than the treatment groups.
Replication	All experiments were performed in 2-5 independent experiments, with sample sizes defined as biological replicates. In some cases, experiments were performed by two independent laboratories (Brestoff Lab at WashU and Yokota at Osaka University) and all data were pooled to generate the final dataset.
Randomization	Mice were randomly assigned to treatment groups.
Blinding	The person performing the assays were sometimes but not always blinded to treatment group. Typically, experiments were managed and treatments were performed by one individual, and the neurologic, behavioral, and/or metabolic cage assays were managed and performed by another individual who was blinded to the group assignments or who was unaware of the ear tag until after the assay was completed. However, in many cases, it was possible to identify mice in the treatment groups because mitochondria-treated mice appeared more robust, had improved reflexes, and had differential hair growth compared to the control mice. This precluded strict blinding.

## Reporting for specific materials, systems and methods

We require information from authors about some types of materials, experimental systems and methods used in many studies. Here, indicate whether each material, system or method listed is relevant to your study. If you are not sure if a list item applies to your research, read the appropriate section before selecting a response.



## Materials &amp; experimental systems

n/a	<input type="checkbox"/>	Involvement in the study
<input checked="" type="checkbox"/>	<input checked="" type="checkbox"/>	Antibodies
<input type="checkbox"/>	<input checked="" type="checkbox"/>	Eukaryotic cell lines
<input checked="" type="checkbox"/>	<input type="checkbox"/>	Palaeontology and archaeology
<input type="checkbox"/>	<input checked="" type="checkbox"/>	Animals and other organisms
<input checked="" type="checkbox"/>	<input type="checkbox"/>	Clinical data
<input checked="" type="checkbox"/>	<input type="checkbox"/>	Dual use research of concern
<input checked="" type="checkbox"/>	<input type="checkbox"/>	Plants

## Methods

n/a	<input type="checkbox"/>	Involvement in the study
<input checked="" type="checkbox"/>	<input type="checkbox"/>	ChIP-seq
<input type="checkbox"/>	<input checked="" type="checkbox"/>	Flow cytometry
<input checked="" type="checkbox"/>	<input type="checkbox"/>	MRI-based neuroimaging

## Antibodies

## Antibodies used

BV421 CD41 (MWReg30, Biolegend, 1:300)  
 PB TER-119 (TER-119, Biolegend, 1:300)  
 PerCP-Cy5.5 CD45 (30-F11, Biolegend, 1:200)  
 Mouse Fc Block (anti-CD16/32, BD Pharmingen)  
 PE/Cy7-CD45.2 (clone 104, Biolegend, dilution factor 1:200)  
 APC-CD45.1 (clone A20, Biolegend, 1:200)  
 PerCP-CD45 (30-F11, Biolegend, 1:200)  
 BV421-SiglecF (E50-2440, BD, 1:400)  
 Spark-NIR685-CD19 (6D5, Biolegend, 1:300)  
 BV750-B220 (RA3-6B2, Biolegend, 1:300)  
 APC/Fire810-NK1.1 (S17016D, Biolegend, 1:300)  
 AF488-TCR $\beta$  (H57-597, Biolegend, 1:300)  
 PE/Fire640-CD4 (GK1.5, Biolegend, 1:300)  
 SB550-CD8 (53-6.7, Biolegend, 1:300)  
 PB-CD11b (M1/70, Biolegend, 1:400)  
 BV711-Ly6G (1A8, Biolegend, 1:300)  
 AF700-Ly6C (HK1.4, Biolegend, 1:300)

## Validation

The antibodies used are common reagents and have validation documentation available at the vendors websites. All are validated for use in flow cytometry applications. All antibodies are validated by the manufacturers to detect the indicated antigens of mouse origin.

## Eukaryotic cell lines

Policy information about [cell lines and Sex and Gender in Research](#)

## Cell line source(s)

HeLa cells were obtained from the JCRB Cell Bank (cell number JCRB9004)

## Authentication

None of the cell lines were authenticated.

## Mycoplasma contamination

Cells were not tested for Mycoplasma contamination.

Commonly misidentified lines  
(See [ICLAC](#) register)

No commonly misidentified cell lines were used.

## Animals and other research organisms

Policy information about [studies involving animals; ARRIVE guidelines](#) recommended for reporting animal research, and [Sex and Gender in Research](#)

## Laboratory animals

Experiments performed at Washington University School of Medicine (WUSM) utilized the following mouse strains procured from Jackson Laboratories (Jax): wildtype C57BL6/J (strain number 000664), CD45.1 (Ptrpca, strain number 002014), PhAMexcised (also known as mtDendra2 or mtD2, strain number 018397), and Ndufs4+/- (strain number 027058), and New Zealand Black (also known as NZB/BINJ or NZB, strain number 000684). CD45.1 mtD2+/- mice were generated by crossing mtD2 mice onto a CD45.1 homozygous background. The other strains are on a CD45.2 background. Experiments performed at Osaka University (OU) utilized the following mouse strains procured from Clea Japan: wildtype C57BL6/J, Ndufs4+/- (Jackson Labs via LUCA Science, Inc.), and CD45.1 (Jackson Labs). All mice were on a C57BL6/J background, except for NZB mitochondria donors. Ndufs4+/- mice were generated by crossing heterozygous males and females from Jackson Labs stock as duos (1 female and 1 male) or trios (2 females and 1 male per cage), with timed breeding to generate many litters born within a few days of each other. Heterozygotes from that cross were used for subsequent breeding. All mice were housed in a Specific Pathogen Free (SPF) barrier facility at room temperature with a 12h:12h light:dark cycle, with lights on at 6am and lights off at 6pm, and had access to food and water ad libitum. The animal facilities were maintained at room temperature (range of 20-26 °C at WashU, range of 21.5-24.5 °C at Osaka University) with a target humidity setpoint of 30-70% at WashU and 45-65% at Osaka University. Male and female Ndufs4+/- mice were used interchangeably and in similar proportions with treatment starting at age 3-5-weeks-old. True survival was determined as the actual date of death minus the date of birth without using euthanasia criteria. This method is used to determine survival because some euthanasia criteria are subjective and/or transient (e.g. immobility) or do not reflect future lifespan accurately (e.g., low core body

temperature). In order to harvest tissues, separate experiments were performed from survival curve studies, and mice were euthanized using isoflurane asphyxiation before tissue procurement. In some cases, tail vein blood was collected from awake mice.

#### Wild animals

The study did not involve wild animals.

#### Reporting on sex

Ndufs4<sup>-/-</sup> males and females were used interchangeably. For bone marrow transplants, male bone marrow was transplanted into male recipients, and female bone marrow was transplanted into female recipients.

#### Field-collected samples

The study did not involve specimens collected in the field.

#### Ethics oversight

Studies performed at Washington University School of Medicine were approved under Institutional Animal Care and Use Committee (IACUC) protocol 22-0286. Studies performed at Osaka University were approved by the Institutional Animal Care and Use Committee at Osaka University Graduate School of Medicine (Approval number: 30-096-013).

Note that full information on the approval of the study protocol must also be provided in the manuscript.

## Flow Cytometry

### Plots

Confirm that:

- The axis labels state the marker and fluorochrome used (e.g. CD4-FITC).
- The axis scales are clearly visible. Include numbers along axes only for bottom left plot of group (a 'group' is an analysis of identical markers).
- All plots are contour plots with outliers or pseudocolor plots.
- A numerical value for number of cells or percentage (with statistics) is provided.

### Methodology

#### Sample preparation

Flow cytometric detection of extracellular mitochondria in blood  
Peripheral blood was sampled from the tail vein, and 5  $\mu$ L blood was transferred to 245  $\mu$ L ACK RBC Lysis Buffer containing 1 mg/mL heparin (Grade 1A, Sigma-Aldrich) with gentle mixing. The cells were pelleted by centrifugation at 500 x g at 4  $^{\circ}$ C for 5 min. The cell-free supernatant was collected (200  $\mu$ L, equal to 80% of the total volume) for small-particle flow cytometry to detect extracellular mitochondria in blood, as previously described.<sup>4</sup> In brief, the cell-free fraction was pelleted at 15,000 x g at 4  $^{\circ}$ C for 5 min, and the supernatant was removed prior to resuspension in 1 mL PBS. The cell-free fraction was pelleted as described and resuspended in 50  $\mu$ L staining buffer containing the following antibodies: BV421-CD41 (MWReg30, Biolegend, dilution factor 1:300), PB-TER-119 (TER-119, Biolegend, 1:300), PerCP/Cy5.5-CD45 (30-F11, Biolegend, 1:200). The particles were washed by adding 1 mL FACS Buffer (PBS containing 2.5% heat-inactivated FBS and 2.5 mM EDTA followed by filter-sterilization) and centrifuging the samples at 15,000 x g at 4  $^{\circ}$ C for 5 min. The pelleted particles were resuspended in a final volume of 200  $\mu$ L FACS buffer, and flow cytometry was performed on a 4-laser Cytex (16V-14B-10YG-8R configuration using SpectroFlo v2.0 software) with small particle settings (FSC = 675, SSC = 235-255, threshold = 6,000). Submicron size calibration beads loaded with FITC (ThermoFisher) were used to identify particles under 2 microns and to set gains to detect the smallest possible particles, with a 300 nM lower limit of detection for this cytometer. We then acquired 100  $\mu$ L of each specimen. Extracellular mitochondria were defined as CD45<sup>-</sup> CD41<sup>-</sup> TER-119<sup>-</sup> particles <2 microns in diameter and mtD2<sup>+</sup>. Mitochondria percentages were defined as the percentage of all CD45<sup>-</sup> CD41<sup>-</sup> TER-119<sup>-</sup> particles that were mtD2<sup>+</sup>. Cell-free mitochondria counts in 1 mL of blood were defined as total mtD2<sup>+</sup> events x 2 (to account for acquiring half the stained specimen) x 1.25 (to account for processing 80% of the original specimen's volume) x 200 (to account for collecting 5  $\mu$ L of whole blood).

#### Flow cytometric analyses of cells

In some cases, peripheral blood from the tail vein was collected, as described in the section on flow cytometric detection of cell-free mitochondria in blood, however pelleted cells were collected for processing. Mice were perfused with 10 mL PBS, as described above, and the spleens and livers were dissected. Spleen cells were obtained by mashing them through a 100- $\mu$ m cell strain using a sterile syringe plunger and washed with Wash Media. To isolate cells from the bone marrow (BM), the soft tissue was removed from the femur and tibia. The ends of each bone were cut and bones were placed in 0.5 mL tubes that had holes poked through the bottom using a 16G needle, and then placed within 1.5 mL tubes. To extract BM, bones were centrifuged at 500 x g at 4  $^{\circ}$ C for 1 min, and pelleted BM was resuspended in Wash Media. Liver non-parenchymal cells were isolated by finely mincing the livers using a razor blade and processed according to established protocols.<sup>40</sup> Briefly, minced livers were digested in high glucose DMEM containing 0.75 mg/mL collagenase A (Sigma) and 50  $\mu$ g/mL DNase I (Sigma) for 30 min in an orbital shaker at 140 rpm at 37  $^{\circ}$ C. Liver digests were centrifuged at 50 x g at 4  $^{\circ}$ C for 3 min to pellet hepatocytes. Supernatant containing non-parenchymal cells was carefully pipetted into a fresh conical tube. Splenic, liver, and BM non-parenchymal cells were resuspended in 1-2 mL ACK RBC Lysis Buffer and incubated at room temperature for 5 min. The reaction was quenched by adding 10 mL Wash Media. The cells were pelleted and collected in 96-well round-bottom plates for staining. The cells from blood, spleen, liver, and/or bone marrow were spun in a swinging bucket centrifuge at 500 x g at 4  $^{\circ}$ C for 5 min, and the supernatants were flicked off. Cells were washed once in 200  $\mu$ L PBS, followed by immediate centrifugation at 500 x g at 4  $^{\circ}$ C for 3 min. The supernatants were discarded, and the cells were resuspended in 50  $\mu$ L PBS containing Zombie NIR viability dye (1:1,000 in PBS, BioLegend) and incubated on ice for 5 min. The reaction was quenched by adding 200  $\mu$ L FACS Buffer. The cells were pelleted at 500 x g at 4  $^{\circ}$ C for 5 min, and then resuspended in 25  $\mu$ L Mouse BD Fc Block (anti-CD16/32, BD Pharmingen) at 1:100, diluted in FACS Buffer. After 15 min on ice, a 25  $\mu$ L aliquot of a 2X antibody cocktail in Brilliant Stain Buffer (BD) was added to the cells and mixed by gently pipetting up and down. The cells were stained with PE/Cy7-CD45.2 (clone 104, Biolegend, dilution factor 1:200) and APC-CD45.1 (clone A20, Biolegend, 1:200) to separate donor and host immune cells. Immune cell populations were further characterized with the following antibodies:

	PerCP-CD45 (30-F11, Biolegend, 1:200), BV421-SiglecF (E50-2440, BD, 1:400), Spark-NIR685-CD19 (6D5, Biolegend, 1:300), BV750-B220 (RA3-6B2, Biolegend, 1:300), APC/Fire810-NK1.1 (S17016D, Biolegend, 1:300), AF488-TCR $\beta$ (H57-597, Biolegend, 1:300), PE/Fire640-CD4 (GK1.5, Biolegend, 1:300), SB550-CD8 (53-6.7, Biolegend, 1:300), PB-CD11b (M1/70, Biolegend, 1:400), BV711-Ly6G (1A8, Biolegend, 1:300), AF700-Ly6C (HK1.4, Biolegend, 1:300). Cells were stained for 30 min on ice and then washed twice with 200 $\mu$ L FACS Buffer prior to final resuspension in a volume of 200 $\mu$ L. For each specimen, 100 $\mu$ L cell suspension was acquired on a Cytex Aurora (SpectroFlo v2.0 software). Analyses of flow cytometry data were conducted with FlowJo (BD) version 10.8 or 10.9 software.
Instrument	Cytex Aurora (4 lasers: V16-B14-YG10-R8)
Software	SpectroFlo v2.0, FlowJo v10.8 or v10.9.
Cell population abundance	Cell populations are defined as % of live, % of parent gate, or numbers of cells per gram of tissue (or per mL blood). The reported parameters are specified clearly in the text and figure legends. Cell-free mitochondria counts in 1mL of blood were defined as total mtD2+ events x 2 (to account for acquiring half the stained specimen) x 1.25 (to account for processing 80% of the original specimen's volume) x 200 (to account for collecting 5 $\mu$ L of whole blood). The Cytex Aurora is a volumetric device, therefore events acquired are an accurate estimate of their true abundance.
Gating strategy	<p>For cells, we gated on cells in the FSC-A x SSC-A gate and then defined singlets using a FSC-A x FSC-H plot. We then gated on live cells using ZombieNIR. We then showed CD45.1 x CD45.2 to identify donor and host immune cells. The CD45.1+ CD45.2- donor cells were gated on and overlaid on top of CD45.1- CD45.2+ host radioresistant immune cells to generate histograms (modal normalization) reporting mtD2 signal. Radioresistant host immune cells were further defined as NK1.1- TCRbeta+ T cells, B220+ CD19+ B cells, Ly6G+ Ly6C- neutrophils, or Ly6G- Ly6C+ monocytes. Host non-immune cells were defined as CD45.1- CD45.2- cells that were further delineated as EpCAM+ CD31- epithelial cells, EpCAM- CD31+ endothelial cells, or EpCAM- CD31- stromal cells.</p> <p>In mitochondria transplant studies, we used a similar gating strategy to define each immune cell population using CD45+ to define immune cells. Furthermore, in those studies NK cells were defined as NK1.1+ TCRbeta- cells, eosinophils were defined as SiglecF+ SSC-A(high), monocytes were defined as Ly6G- Ly6C+ CD11b+ cells, and TCRbeta+ T cells were further defined as CD4+ CD8- and CD4- CD8+ T cell subsets.</p> <p>For cell-free mitochondria (isolated or in blood), we put the FSC-A and SSC-A plots on the log scale (events collect with FSC voltage at 675 mV, so cells are off-scale), and we used size calibration beads to set the gates to be inclusive of all events under 2 microns that could be detected above noise (threshold set at 6,000). We then excluded all CD41+, CD45+, and TER-119+ events via sequential negative gating to identify all lineage-negative submicron particles devoid of platelets, immune cell fragments, and red blood cell fragments, respectively. We then plotted mtD2 against TER-119 to show mtD2+ events, which we gated using guidance from contour plots.</p> <p>All gating strategies are provided in the Supplementary Information.</p>

Tick this box to confirm that a figure exemplifying the gating strategy is provided in the Supplementary Information.